Response to Reviewers comments for
Aqueous Reactions of Organic Triplet Excited States with Atmospheric Alkenes
By Richie Kaur et. al.

Please note:
Reviewer comment is in black text.
Our response is in blue.

Please note that line numbers in the revised version are different due to changes in the manuscript.

Anonymous Referee #1
Received and published: 4 February 2019

Major comment: The authors present a nice study on the reactions of a model triplet species with various alkenes and reveal which features (e.g. one electron reduction potential, double bond location) have a higher reactivity towards triplets. When reading the manuscript, I was curious whether or not the authors could confirm that the rate constants for triplet benzophenone are similar to those generated from brown carbon/ natural organic matter (NOM). Although beyond the scope of this study, a discussion of how the rate constants for the 17 model compounds might be different for triplet NOM, or how they might vary if NOM is also present, might be useful.

We thank this reviewer for their thorough review and detailed, helpful comments. Based on our two studies to date, NOM triplets in fog and airborne particles are about as reactive as the triplets of 3'-methoxyacetophenone (3MAP) and 3,4-dimethoxybenzaldehyde (DMB). For the few alkenes where there are rate constants for both these triplets and triplet benzophenone, the latter is approximately 25 times more reactive. This information is in Section 3.4 of the manuscript.

Minor comments:

1. Abstract/Intro Is brown carbon something that needs to be defined here (like in line 46)? Or is it a fairly common term in atmospheric chemistry literature?

The reviewer is correct – brown carbon is a fairly common term used in atmospheric chemistry. However, taking the reviewer's question into account, we have included a brief description in the abstract in line 13.

2. Is "a.k.a" commonly used?

This refers to line 13 (first line of the abstract). We think it is a commonly used abbreviation, but we have replaced it with "or" to avoid any confusion.

3. Line 76: what are the steady-state concentrations of OH radicals and triplets? Are the concentrations of benzophenone and alkenes used in this study environmentally relevant?

For this study, our goal was to measure rate constants for the BP triplet with alkenes, which does not require that the triplet concentration is environmentally relevant. Since we used a relative-rate approach, initial concentrations of the reactants do not impact the outcome. But to answer the question, we estimate that $^3C^*$ concentrations in our solutions are 10^{-14} to 10^{-15} M (see answer to Q5 for more details) which is similar to fog triplet concentrations (Kaur and Anastasio, 2018). In comparison, our alkene concentrations are probably higher, by a factor of at least 10, compared to a fog drop. (But, as stated earlier, this does not impact our determination of the rate constant.)

Some hydroxyl radical ($^•OH$) was probably generated during our experiments. However, we estimate that the $^•OH$ concentration is small and has no significant impact on our rate constants; we discuss this issue in more detail in response to question 5 below.

4. Methods. Why was a pH of 5.5 selected?

The pH of 5.5 was based on the average pH we measured in fog waters in a recent study of 5.6 ($\pm$ 0.9) (Kaur and Anastasio, 2017). We have added this information in line 101.

5. Does irradiating the benzophenone solution generate other oxidants? Can you confirm all reactions due to 3BP*? Similarly, do any of the test alkenes or reference compounds degrade due to direct photoreactions when BP is not present?

This is a good question. The two most likely other oxidants formed in our system are singlet oxygen ($^1O_2^*$) and hydroxyl radical ($^•OH$).

$^1O_2^*$ is formed by reaction of triplets with O_2 (Zepp et al., 1977; Haag and Hoigné, 1986); for $^3BP^*$, the $^1O_2^*$ yield (i.e., f_Δ) for this reaction is 0.35 (Wilkinson et al., 1993). Based on our measured alkene decays, the triplet BP concentration in our solutions was typically 1×10^{-15} M. As described by McNeill and Canonica (2016), the singlet oxygen concentration can be estimated by

$$[^1O_2^*] \approx 2 f_\Delta [^3C^*]$$

For ^{3}BP* this gives a singlet oxygen concentration of nearly 1×10^{-15} M. For the three alkenes (HxAc, HxO, and MeJA) where we have rate constants with both ^{3}BP* (this work) and ^{1}O$_2$* (Richards-Henderson et al., 2014b), the average value of $k_{\text{ALK+1O2*}} / k_{\text{ALK+3BP*}}$ is 4.0×10^{-4}; i.e., rate constants for alkenes with triplet BP are approximately 2500 times faster than with singlet oxygen. Thus, since the concentrations of ^{3}C* and ^{1}O$_2$* are likely similar in our solutions but ^{1}O$_2$* reacts much more slowly with alkenes, singlet oxygen should be a negligible sink for the alkenes in our experiments. We have added this idea to the end of section 2.2.

In the case of $^\bullet$OH, we cannot estimate its formation rate or steady-state concentration, which makes it impossible to quantify its contribution to alkene loss. However, there is at least one piece of evidence that argues against $^\bullet$OH as a significant oxidant in our samples. $^\bullet$OH reacts with most alkenes at very similar, near diffusion-controlled, rates. For example, the second-order rate constants for $^\bullet$OH with allyl alcohol (AlO) and methyl jasmonate (MeJA) are 6.0×10^9 M^{-1} s^{-1} (Simic et al., 1973) and 6.7×10^9 M^{-1} s^{-1} (Richards-Henderson et al., 2014a), respectively. This is a difference of only 11%. In contrast, our measured rate constant for MeJA with ^{3}BP* is more than 30 times higher than the value for AlO with ^{3}BP*. This suggests that $^\bullet$OH has no significant impact on our measured rate constants.

Finally, direct photodegradation of all alkenes was examined in illuminated solutions without BP: no direct loss was detected for any of the compounds. We added this information to section 2.2.

6. How does 100 uM BP and 50 uM alkene compare to brown carbon concentrations and alkene concentrations, respectively, in fog droplets/aqueous particles?

Dissolved organic carbon concentrations can range between 1200 and 2700 μM-C in Davis fog drops (Anastasio and McGregor, 2001; Zhang and Anastasio, 2001; Kaur and Anastasio, 2017) and can be several orders of magnitude higher in particles. As for the alkenes, we haven't seen concentrations reported, but they are probably at least 10 times lower than our concentration. However, as mentioned above, when determining rate constants with the relative rate method the species do not need to be at atmospherically relevant concentrations.

7. What irradiation time or times were used? Did they vary?

Irradiation times were typically between 60 and 150 minutes, with the length dependent upon the reactivity of the alkene. We have included a statement about this in Section 2.2.

8. Is oxygen consumed in sealed quartz cell during this time, impacting rates?

We do not think there was significant consumption of dissolved O_2 since the solutions started saturated with air (corresponding to 284 µM of dissolved O_2) and the cell was opened multiple times during illumination when aliquots were removed. If dissolved oxygen had been significantly consumed during the course of the experiments, the concentration of BP triplet would have increased since O_2 is the main sink of triplets. In that case, the rate constants for loss of alkene and reference compound would have increased with illumination time. We did not observe this: the loss of alkenes and reference compounds were always first order and the slope of the $\ln(C/C_0)$ vs. time plot did not change with time. Thus, our evidence indicates that oxygen was not significantly consumed during the experiments.

9. I imagine benzophenone and NOM have different absorbance (A) spectra? It would be interesting to compare A spectra multiplied by irradiance for benzophenone and for brown carbon (or something similar to figure S1).

   While these action spectra for light absorption would be interesting, whether the BP and NOM results are similar or different wouldn't have any effect on our results. This is an interesting question, but it does not fit within the scope of our study.

10. Fig. S1 is a bit confusing showing %transmittance for the light source and not its irradiance through the filters? I think showing the irradiance the sample sees would be more useful for a comparison to solar irradiation. I imagine the photon dose the sample sees impacts the formation of triplets, can the authors confirm that this does this not matter for the competition kinetic experiments performed here?

   We thank the reviewer for this feedback. We measured the irradiance of our system and used this data to revise Figure S1 as:
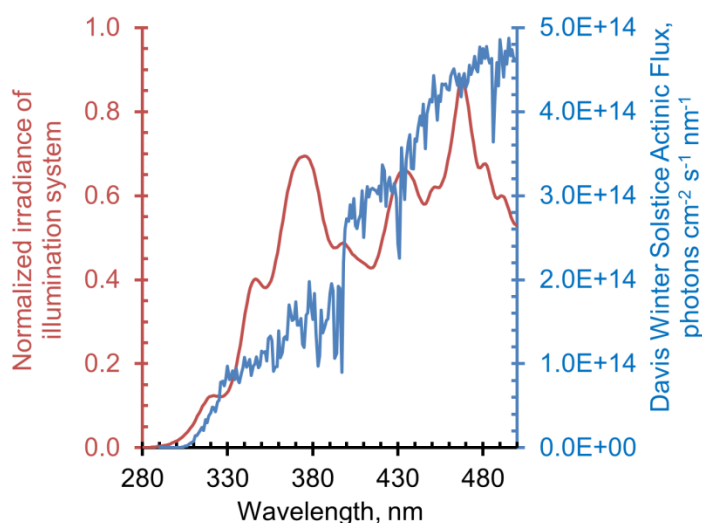
Since we are using a relative rate method, where both the reference compound and test alkene are seeing the same concentration of ^{3}BP*, regardless of changes in lamp flux, the irradiance does not affect the second-order rate constant that we determine. While absolute loss rates of the test and reference species are affected by the photon dose, the ratio of pseudo-first-order reaction rate constants are independent of photon flux.

11. Line 115-117: Where was the aluminum wrapped dark in relation to the irradiated sample? If the two samples are side by side there will certainly be issues since aluminum foil is a hard reflector and could increase photon dose in irradiated sample.

We appreciate the reviewer's thoughtfulness here. The aluminum-wrapped "dark" cuvette and the illuminated sample were in the same chamber but not kept side by side. The dark cuvette was placed in a corner, not in the path of the light beam so that it was subjected to the same temperature and other conditions as the illuminated sample. We have included this clarification in the Section 2.2.

12. Results/Discussion Lines 311-333: As the authors note, adjusting 3BP* constants is uncertain, but I also now wonder if 3MAP and DMB triplets are more representative of triplets from NOM? Or is that unknown?

Based on our recent work (the only two studies that have measured triplets in atmospheric samples, as best we know), the NOM triplets in fog and PM are typically most similar to ^{3}3MAP* and ^{3}DMB*. This is why we adjusted the ^{3}BP* rate constants to what we would expect for an average of ^{3}3MAP* and ^{3}DMB*. This is described in Section 3.4.

Anonymous Referee #2
Received and published: 6 February 2019

In this very ambitious study, the authors measured the kinetics of oxidation of a series of alkenes by the triplet excited state of benzophenone, which they use as a model compound for triplet excited states in atmospheric waters. They then looked for correlations between the kinetic data and various properties of the alkenes, some of which were derived using density functional theory (DFT) calculations. They found a fairly good correlation between the rate constants and the one-electron oxidation potential for the alkenes, and used that to develop a quantitative structure-activity relationship (QSAR). They used the QSAR, and more DFT calculations, to infer triplet oxidation rates for several biogenically derived alkenes. Finally, they perform some estimates of the potential importance of triplet chemistry in atmospheric waters. I recommend publication in ACP after some minor points are addressed.

We thank this reviewer for their thoughtful review, encouraging comments, and specific suggestions for improvement of the manuscript.

Minor comments:
1. - It is not mentioned in the main text how many times each kinetic experiment was repeated - I only knew this after looking at Table S1.

We have added this information to Section 2.2.

2. - Can the authors discuss and provide some estimate of the error/uncertainty for the parameters derived from the DFT calculations? How does this impact the discussion of the outliers for the QSAR?
We think the reviewer is inquiring about the CBS-QB3 method specifically, as this was the method used for calculations of BDEs, BDFEs, and OPs. In the article describing this method, the authors state that the errors for CBS-QB3 have a mean absolute deviation of 1.10 kcal/mol on a test set they used. This is comparable to other post-Hartree-Fock ab initio methods (such as MP2, a method we used to calculate HOMOs/SOMOs), which have mean absolute deviations of 0.94 -1.21 kcal/mol on the same test set. This error of roughly 1 kcal/mol corresponds to only 0.04 V in OP, so does not account for the over- or under-prediction of the outliers in Figure 3, which are off by greater amounts. We have added a description of these errors to Section 2.3.

3. I note from Table S1 that several different reference probes were used. The reason for this should be discussed. The reference rates and the uncertainty in those rates should be listed/discussed. Were the uncertainties included in the reported uncertainties in k,

6

and considered in the development of the QSAR?

We used several probes so that the loss rates of the test and references alkenes were similar. If the loss rates are very different it is difficult to get good rate constants for both species during the same illumination time. The reference rates and the uncertainties are given in Table S1. We have included a statement about this in Section 2.2.

The standard errors in the slope and reference rate constant were propagated to obtain the uncertainties listed for each replicate in parentheses in Table S1. Since each experiment was performed in triplicate, we used the standard deviation of the mean for the QSAR Figure 3. The uncertainties were not considered in the development of the QSAR.

4. - Just a suggestion: Fig. 4 and some of the discussion of these calculations could be moved to the SI, since the article is already quite dense with information and this line of inquiry was ultimately inconclusive.

We appreciate the reviewer's comment about the article being dense with information. However, we feel that Figure 4 provides a good example of the computational work that was performed and illustrates an interesting difference in the reactivity of the alkenes we studied. Even though the transition state structures and associated thermodynamics didn't end up being predictive of rate constants, we have kept the figure in the main text because this is an important negative result.

5. - A little more information about the atmospheric lifetime calculations should be provided. Are you considering repartitioning of the OVOCs between the gas and aqueous phases as the reaction proceeds? Or are the calculated rates basically initial rates?

This is a good question. Since we are only providing rough estimates, we have not considered repartitioning of the OVOCs between the phases and only considered the initial rates. We added a clarifying "initial" in the first paragraph of Section 3.4.

References

Anastasio, C., and McGregor, K. G.: Chemistry of fog waters in California's central valley: 1. In situ photoformation of hydroxyl radical and singlet molecular oxygen, Atmos. Environ., 35, 1079-1089, 2001.

Haag, W. R., and Hoigné, J.: Singlet oxygen in surface waters .3. Photochemical formation and steady-state concentrations in various types of waters, Environ. Sci. Technol., 20, 341-348, 1986.

Kaur, R., and Anastasio, C.: Light absorption and the photoformation of hydroxyl radical and singlet oxygen in fog waters, Atmos. Environ., 164, 387-397, 2017.

Kaur, R., and Anastasio, C.: First Measurements of Organic Triplet Excited States in Atmospheric Waters, Environ. Sci. Technol., 52, 5218-5226, 2018.

McNeill, K., and Canonica, S.: Triplet state dissolved organic matter in aquatic photochemistry: Reaction mechanisms, substrate scope, and photophysical properties, Environ. Sci. Process. Impact., 18, 1381-1399, 2016.

Richards-Henderson, N. K., Hansel, A. K., Valsaraj, K. T., and Anastasio, C.: Aqueous oxidation of green leaf volatiles by hydroxyl radical as a source of SOA: Kinetics and SOA yields, Atmos. Environ., 95, 105-112, 2014a.

Richards-Henderson, N. K., Pham, A. T., Kirk, B. B., and Anastasio, C.: Secondary Organic Aerosol from Aqueous Reactions of Green Leaf Volatiles with Organic Triplet Excited States and Singlet Molecular Oxygen, Environmental Science & Technology, 49, 268-276, 2014b.

Simic, M., Neta, P., and Hayon, E.: Reactions of hydroxyl radicals with unsaturated aliphatic alcohols in aqueous solution. Spectroscopic and electron spin resonance radiolysis study, J. Phys. Chem., 77, 2662-2667, 1973.

Wilkinson, F., Helman, W. P., and Ross, A. B.: Quantum yields for the photosensitized formation of the lowest electronically excited singlet state of molecular oxygen in solution, J. Phys. Chem. Ref. Data, 22, 113-262, 1993.

Zepp, R. G., Wolfe, N. L., Baughman, G. L., and Hollis, R. C.: Singlet oxygen in natural waters, Nature, 267, 421-423, 1977.

Zhang, Q., and Anastasio, C.: Chemistry of Fog Waters in California's Central Valley—Part 3: Concentrations and Speciation of Organic and Inorganic Nitrogen, Atmos. Environ., 35, 5629-5643, 2001.

1 **Aqueous Reactions of Organic Triplet Excited States with Atmospheric**

2 **Alkenes**

3 Richie Kaur [a,b], Brandi M. Hudson [c], Joseph Draper [a, #], Dean J. Tantillo [c], and Cort Anastasio [*a,b]

4 [a] Department of Land, Air, and Water Resources, University of California, Davis, California
5 95616, United States
6 [b] Agricultural & Environmental Chemistry Graduate Group, University of California, Davis
7 [c] Department of Chemistry, University of California, Davis, California 95616, United States
8 [#] Now at the Fresno Metropolitan Flood Control District, Fresno, California 93727, United
9 States
10 Correspondence to: C. Anastasio (canastasio@ucdavis.edu)
11

12 Abstract

13 Triplet excited states of organic matter are formed when colored organic matter (i.e., brown

14 carbon) absorbs light. While these "triplets" can be important photooxidants in atmospheric

15 drops and particles (e.g., they rapidly oxidize phenols), very little is known about their reactivity

16 toward many classes of organic compounds in the atmosphere. Here we measure the bimolecular

17 rate constants of the triplet excited state of benzophenone (^{3}BP*), a model species, with 17

18 water-soluble $C_3 - C_6$ alkenes that have either been found in the atmosphere or are reasonable

19 surrogates for identified species. Measured rate constants ($k_{ALK+3BP*}$) vary by a factor of 30 and

20 are in the range of $(0.24 - 7.5) \times 10^9 \, M^{-1} \, s^{-1}$. Biogenic alkenes found in the atmosphere – e.g.,

21 cis-3-hexen-1-ol, cis-3-hexenyl acetate, and methyl jasmonate – react rapidly, with rate constants

22 above $1 \times 10^9 \, M^{-1} \, s^{-1}$. Rate constants depend on alkene characteristics such as the location of the

23 double bond, stereochemistry, and alkyl substitution on the double bond. There is a reasonable

24 correlation between $k_{ALK+3BP*}$ and the calculated one-electron oxidation potential (OP) of the

25 alkenes ($R^2 = 0.58$); in contrast, rate constants are not correlated with bond dissociation

26 enthalpies, bond dissociation free energies, or computed energy barriers for hydrogen

27 abstraction. Using the OP relationship, we estimate aqueous rate constants for a number of

28   unsaturated isoprene and limonene oxidation products with $^3BP^*$: values are in the range of

29    $(0.080–1.7) \times 10^9 \ M^{-1} \ s^{-1}$, with generally faster values for limonene products. <u>Rate constants</u>

30   <u>with less reactive triplets, which are probably more environmentally relevant, are likely roughly</u>

31   <u>25 times slower.</u> Using our predicted rate constants, along with values for other reactions from

32   the literature, we conclude that triplets are probably minor oxidants for isoprene and limonene-

33   related compounds in cloudy or foggy atmospheres, except in cases where the triplets are very

34   reactive.

35

1   Introduction

37   Photochemical processes in atmospheric aqueous phases (e.g., cloud and fog drops and

38   aqueous particles) are important sources and sinks of secondary organic species (Blando and

39   Turpin, 2000; Lim et al., 2010; Kroll and Seinfeld, 2008; Volkamer et al., 2009; Gelencsér and

40   Varga, 2005), which represent a large fraction of aerosol mass (Zhang et al., 2007; Hallquist et

41   al., 2009). Many of these reactions involve photooxidants, including hydroxyl radical ($^{\bullet}OH$),

42   which is widely considered to be the dominant aqueous oxidant (Herrmann et al., 2010;

43   Herrmann et al., 2015). But there are numerous other aqueous photooxidants, such as singlet

44   molecular oxygen, hydroperoxyl radical/superoxide radical anion, hydrogen peroxide, and triplet

45   excited states of organic matter ($^3C^*$ or triplets) (Lee et al., 2011; Anastasio and McGregor,

46   2001; Kaur and Anastasio, 2017; Anastasio et al., 1996; Anastasio et al., 1994; Zepp et al., 1977;

47   Wilkinson et al., 1995; Kaur and Anastasio, 2018). Formed from the photoexcitation of colored

48   organic matter (i.e., brown carbon), triplets are important oxidants in surface waters for several

49   classes of organic compounds, including phenols, anilines, amines, phenylurea herbicides, and

50   heterocyclic sulfur-containing compounds (Canonica et al., 1995; Canonica and Hoigné, 1995;

51   Arnold, 2014; Canonica et al., 2006a; Bahnmüller et al., 2014; Boreen et al., 2005); however,

52   very little is known about atmospheric triplets.

53   Recent studies have shown that aqueous triplets can be the dominant oxidants for phenols

54   emitted during biomass combustion (Smith et al., 2014), with phenol lifetimes on the order of a

55   few hours in fog drops (Kaur and Anastasio, 2018) and aqueous particle extracts (Kaur et al.,

56   2018).There is also evidence that triplets can oxidize some unsaturated aliphatic compounds.

57   Richards-Henderson et. al.(Richards-Henderson et al., 2014b) measured rate constants for five

58   unsaturated biogenic volatile organic compounds (BVOCs) with the model triplets 3,4-

59   dimethoxybenzaldhyde and 3'-methoxyacetophenone, and found that rate constants ranged

60   between 10^7 and 10^9 $M^{-1} s^{-1}$. Other laboratory studies have shown that triplet states of

61   photosensitizers such as imidazole-2-carboxaldehyde and 4-benzoylbenzoic acid can oxidize

62   gaseous aliphatic BVOCs, e.g., isoprene and limonene, and model aliphatic compounds, e.g., 1-

63   octanol, at the air-water interface to form low-volatility products that increase particle mass (Fu

64   et al., 2015; Rossignol et al., 2014; Li et al., 2016; Laskin et al., 2015). However, the

65   atmospheric importance of these types of processes are unclear (Tsui et al., 2017). Additionally,

66   we recently reported that natural triplets in illuminated fog waters and particle extracts are

67   significant oxidants for methyl jasmonate, an unsaturated aliphatic BVOC, accounting for 30–80

68   % of its aqueous loss during illumination (Kaur et al., 2018; Kaur and Anastasio, 2018).

69   Abundant BVOCs such as isoprene and limonene are rapidly oxidized in the gas phase to

70   form unsaturated C_3–C_6 oxygenated volatile organic compounds (OVOCs) that include isoprene

71   hydroxyhydroperoxides, isoprene hydroxynitrates, and isoprene and limonene aldehydes (Surratt

72   et al., 2006; Paulot et al., 2009b; Crounse et al., 2011; Ng et al., 2008; Walser et al., 2008; Paulot

73   et al., 2009a). Several of these first-generation products have high Henry's law constants, above

74   10^4 $M atm^{-1}$ (Marais et al., 2016) and partition significantly into cloud and fog drops and, to a

75   smaller extent, into aerosol liquid water. There, they can undergo further oxidation by aqueous

76   photooxidants, including $^\bullet$OH and ozone (Wolfe et al., 2012; St. Clair et al., 2015; Khamaganov

77   and Hites, 2001; Schöne and Herrmann, 2014; Lee et al., 2014) and possibly triplets. Our past

78   measurements have shown that steady-state concentrations of ^{3}C* are orders of magnitude higher

79   than $^\bullet$OH in fog waters and aqueous particles (Kaur et al., 2018; Kaur and Anastasio, 2018) and

80   thus they might contribute significantly to the loss of OVOCs derived from isoprene and other

81   precursors. However, testing this hypothesis requires rate constants for the reactions of triplets

82   with alkenes, which are scarce.

83   To address this gap, we studied the reactions of 17 $C_3 - C_6$ unsaturated compounds with

84   the triplet state of the model compound benzophenone (Fig. 1). While our 17 unsaturated

85   compounds include alcohols, esters, and chlorinated compounds, for simplicity we refer to them

86   all as "alkenes". The tested alkenes include BVOCs emitted into the atmosphere as well as

87   surrogates for some of the small unsaturated gas-phase products formed as secondary OVOCs.

88   The goals of this study are to: 1) measure rate constants for reactions of the alkenes with the

89   triplet excited state of benzophenone, 2) explore quantitative structure-activity relationships

90   (QSARs) between the measured rate constants and calculated alkene properties (e.g., the one-

91   electron oxidation potential) and 3) use a suitable QSAR to estimate rate constants for triplets

92   with some unsaturated isoprene and limonene oxidation products to predict whether or not

93   triplets are significant oxidants for these species in cloud and fog drops.

94

95 **2   Methods**

96 **2.1 Chemicals**

97   All chemicals were purchased from Sigma-Aldrich with purities of 95 % and above, and

98   were used as received: the compound numbers, compound names, and abbreviated names are

99   listed in Table 1. All chemical solutions were prepared using purified water (Milli-Q water) from

100 a Milli-Q Plus system (Millipore; ≥18.2 MΩ cm) with an upstream Barnstead activated carbon

101   cartridge. To mimic fog drop acidity (Kaur and Anastasio, 2017), the pH of each reaction

102   solution was adjusted to 5.5 ($\pm$ 0.2) using a 1.0 mM phosphate buffer.

2.2 Kinetic Experiments

104   Bimolecular rate constants of the alkenes with the triplet state of benzophenone (^{3}BP*)

105   were measured using a relative rate technique, as described in in the literature (Richards-

106   Henderson et al., 2014a; Finlayson-Pitts and Pitts Jr, 1999). The technique involves illuminating

107   a solution containing the triplet precursor (BP), a reference compound with a known second-

108   order rate constant with ^{3}BP*, and one test alkene for which the rate constant is unknown. The

109   reference compound for each alkene was chosen so that the triplet-induced loss rates for test

110   alkene and reference compound were similar. Buffered, air-saturated solutions containing 50 μM

111   each of the reference and test compounds and 100 μM of BP were prepared and then 10 mL of

112   this solution was illuminated in a stirred 2-cm, air-tight quartz cuvette (Spectrocell) at 25 °C.

113   Samples were illuminated with a 1000 W Xenon arc lamp filtered with an AM 1.0 air mass filter

114   (AM1D-3L, Sciencetech) and 295 nm long-pass filter (20CGA-295, Thorlabs) to mimic

115   tropospheric solar light (Fig. S1 of the Supplemental Information). At various intervals, aliquots

116   of illuminated sample were removed and analyzed for the concentration of reference compound

117   and test alkene using HPLC (Shimadzu LC-10AT pump, ThermoScientific BetaBasic-18 C$_{18}$

118   column (250 $\times$ 33 mm, 5 μM bead), and Shimadzu-10AT UV-Vis detector). For each alkene,

119   illumination experiments were performed in triplicate (Table S1), using total illumination times

120   typically between 60 and 150 min. Parallel dark controls were employed with every experiment

121   using an aluminum foil-wrapped cuvette containing the same solution and analyzed in the same

122   manner as the illuminated solutions. The dark cuvette was placed in a corner of the sample

123   chamber, out of the path of the light beam. As a direct photodegradation control, each alkene was

124   also illuminated (separately) in solution without benzophenone; there was no loss for any of the

125   compounds.

126   In every case, loss of test and reference compounds followed first-order kinetics. Plotting

127   the change in concentration of the test alkene against that of the reference compound yields a

128   linear plot that is represented by:

129    $$\ln\frac{[\text{Reference}]_0}{[\text{Reference}]_t} = \frac{k_{\text{Reference}+3BP^*}}{k_{\text{ALK}+3BP^*}} \ln\frac{[\text{ALK}]_0}{[\text{ALK}]_t} \qquad\qquad (1)$$

130   where $[\text{Reference}]_0$, $[\text{Reference}]_t$, $[\text{ALK}]_0$, and $[\text{ALK}]_t$ are the concentrations of the reference

131   and test alkenes at times zero and t, respectively, and $k_{\text{Reference}+3BP^*}$ and $k_{\text{ALK}+3BP^*}$ are the

132   bimolecular rate constants for the reaction of the reference and test alkenes with $^3BP^*$,

133   respectively. A plot of Eq. (1) (with the y-intercept fixed at the origin) gives a slope equal to the

134   ratio of the bimolecular rate constants; dividing $k_{\text{Reference}+3BP^*}$ by the slope gives $k_{\text{ALK}+3BP^*}$. The

135   measurement technique is illustrated in Fig. S2. While $^3BP^*$ makes singlet molecular oxygen

136   ($^1O_2^*$), the latter is an insignificant oxidant of alkenes in our solutions: the concentrations of the

137   two oxidants are similar (McNeill and Canonica, 2016), but our measured rate constants of

138   alkenes with $^3BP^*$ are approximately 2500 times faster than the corresponding rate constants

139   with $^1O_2^*$(Richards-Henderson et al., 2014a).

140   **2.3 Calculation of Oxidation Predictor Variables**

141   All calculations were completed using the Gaussian 09 software suite (Frisch et al.,

142   2009). Structures of alkenes were optimized using uB3LYP/6-31+G(d,p) (Becke, 1992, 1993;

143   Lee et al., 1988; Stephens et al., 1994; Tirado-Rives and Jorgensen, 2008) for reaction coordinate

144   calculations and the CBS-QB3 (Montgomery Jr et al., 1999) method for predicting bond

145   dissociation enthalpies (BDEs), bond dissociation free energies (BDFEs), and oxidation

146   potentials (OPs). This method has a mean absolute deviation of approximately 1 kcal mol^{-1}

147   which corresponds to 0.04 V in E_{ox} (i.e., OP). Transition state structures (TSSs) were optimized

148   in the triplet state using uB3LYP/6-31+G(d,p) (Becke, 1992, 1993; Lee et al., 1988; Stephens et

149   al., 1994; Tirado-Rives and Jorgensen, 2008). TSSs were confirmed by the presence of an

150   imaginary frequency and minima (reactants and products) were confirmed by the absence of

151   imaginary frequencies. Free energy (ΔG) and enthalpy (ΔH) differences were determined by

152   comparing TSS energies relative to their reactant energies. For solvent phase calculations, the

153   solvent model density (SMD) (Marenich et al., 2009) continuum model was used with water as

154   the solvent. To calculate BDEs, the neutral (AH) and radical species ($A^\bullet$) (resulting from H atom

155   abstraction) of each alkene and the H radical ($H^\bullet$) were optimized in the gas phase. Using the

156   computed enthalpies (H) and Eq. (2), the predicted BDEs of each alkene were determined.

157    $BDE = H_{A^\cdot} + H_{H^\cdot} - H_{AH}$ (2)

158   To determine the predicted BDFEs, the neutral (AH_g, AH_{aq}) and radical species ($A^\bullet_g$,

159    $A^\bullet_{aq}$) of each alkene and the H radical ($H^\bullet_g$, $H^\bullet_{aq}$) were optimized in the gas and solvent phases

160   and their differences taken to give $\Delta G^\circ_{solv,AH}$, $\Delta G^\circ_{solv,A}{}^\bullet$, and $\Delta G^\circ_{solv,H}{}^\bullet$, respectively. Based on

161   the thermodynamic cycle shown (Scheme 1), these values were used in Eqs. (3) and (4) to

162   calculate the BDFEs of C–H and O–H bonds.

$$\begin{array}{ccccc}
AH_g & \xrightarrow{\ \Delta G_{rxn,g}\ } & A^\cdot_g & + & H^\cdot_g \\
\Big\downarrow {\scriptstyle \Delta G^o_{solv,A}} & & \Big\downarrow {\scriptstyle \Delta G^o_{solv}} & & \Big\downarrow {\scriptstyle \Delta G^o_{solv}} \\
AH_{aq} & \xrightarrow{\ \Delta G_{rxn,aq}\ } & A^\cdot_{aq} & + & H^\cdot_{aq}
\end{array}$$

163
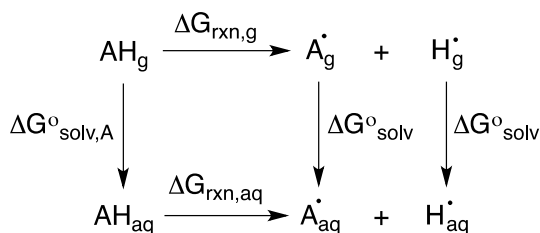
164   **Scheme 1.** Thermodynamic cycle used to calculate bond dissociation free energies.

165    $\Delta\Delta Gsolv = \Delta G^\circ_{solv,A^\cdot} + \Delta G^\circ_{solv,H^\cdot} - \Delta G^\circ_{solv,AH}$ (3)

166    $\Delta G^\circ_{ox} = \Delta G_g + \Delta\Delta G_{solv}$ (4)

167   To predict OPs, the neutral (A_g, A_{aq}) and radical cation ($A^{\bullet+}_g$, $A^{\bullet+}_{aq}$) forms of each alkene

168   were optimized in the gas and solvent phase, their difference giving $\Delta G^\circ_{solv,A}$ and $\Delta G^\circ_{solv,A}{}^\bullet$.

169   Based on the thermodynamic cycle shown below (Scheme 2), these values were used in Eqs. (5–

170   7) to calculate the OP (i.e., E_{ox}) of each alkene.

$$A_g \xrightarrow{IE_{gas}} A_g^{\bullet+} + e_g^-$$

$$\Bigg\downarrow \Delta G^\circ_{solv,A} \qquad \Bigg\downarrow \Delta G^\circ_{solv,A^{\bullet+}} \quad \Bigg\downarrow \Delta G=0$$

$$A_{aq} \xrightarrow{\Delta G^\circ_{ox,aq}} A_{aq}^{\bullet+} + e_g^-$$
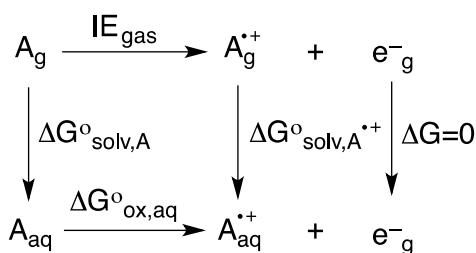
172   **Scheme 2.** Thermodynamic cycle used to calculate oxidation potentials.

173     $$\Delta\Delta G_{solv} = \Delta G^\circ_{solve,A^{\cdot+}} - \Delta G^\circ_{solv,A} \tag{5}$$

174     $$\Delta G^\circ_{ox} = IE_{gas} + \Delta\Delta G_{solv} \tag{6}$$

175     $$E_{ox} = -\left(\frac{-\Delta G^\circ_{ox}}{nF} + SHE\right) \tag{7}$$

176   where n is the number of electrons, F is Faraday's constant (96485.3365 C/mol), and SHE is the

177   potential of the standard hydrogen electrode (4.28 V).

178   Subsequent MP2/CBSB3 (Petersson et al., 1988; Petersson and Al-Laham, 1991;

179   Petersson et al., 1991; Mayer et al., 1998) single point calculations were used to compute the

180   highest occupied molecular orbitals (HOMOs) and singly occupied molecular orbitals (SOMOs).

181   Structural drawings were produced using CYLView (Legault, 2009).

182

183   **3   Results and discussion**

184   **3.1 Alkene-triplet bimolecular rate constants ($k_{ALK+3BP*}$)**

185   Fig. 1 shows the chemical structures for all 17 alkenes and the triplet precursor,

186   benzophenone. The alkenes have molecular weights ranging between 58 and 220 g mol^{-1} and

187   include 13 alcohols, three esters and one chlorinated compound. The model triplet precursor

188   benzophenone (BP) has been previously employed in surface water studies, and its triplet state

189 rapidly reacts with aromatics such as substituted phenols and phenyl urea herbicides with rate

190 constants faster than 10^9 M^{-1} s^{-1} (Canonica et al., 2000; Canonica et al., 2006b).

191   The bimolecular rate constants for the alkenes with the excited triplet state of BP

192 ($k_{\text{ALK+3BP*}}$) vary by a factor of 30, spanning the range of (0.24–7.5) $\times 10^9$ M^{-1}s^{-1}. Values are

193 shown in Tables 1 and S1, and in Fig. S3, where the alkenes are numbered in ascending order of

194 their reactivity towards ^{3}BP*. Based on their rate constants, the alkenes appear to be broadly split

195 into two groups – the slower alkenes (**1–9**), whose rate constants lie below 1×10^9 M^{-1}s^{-1} and

196 span a range of only a factor of 2.5, and the faster alkenes (**10–17**) which vary by a factor of 5.

197 Notably, three of the four BVOCs identified in emissions to the atmosphere – 3MBO (**12**), cHxO

198 (**15**), cHxAc (**16**) and MeJA (**17**) – react rapidly with ^{3}BP*, with rate constants greater than 1 $\times$

199 10^9 M^{-1} s^{-1}.

200   Three alkene characteristics appear to increase reactivity: internal (rather than terminal)

201 double bonds; methyl substitution on the double bond; and alkene stereochemistry. To more

202 specifically examine the impact of these variables, we compare the rate constants for three sets of

203 alkenes (Fig. 2). The lowest free energy and enthalpy barriers for the abstraction of a hydrogen

204 atom are also shown in Fig. 2 (and in Table 1); while overall these computed barriers are not

205 well-correlated with rate constants (discussed below), lower barriers generally correspond to

206 higher rate constants for the sets of alkenes in Fig. 2. The first two sets of compounds in Fig. 2

207 indicate that internal alkenes react faster with ^{3}BP* than do terminal isomers: cHxAc (**16**), an

208 internal hexenyl acetate, has a reaction rate constant 11 times faster than its terminal isomer

209 5HxAc (**9**). The corresponding alcohols also exhibit the same trend: the internal alkenes cHxO

210 (**15**) and tHxO (**10**) react 27 and 5.8 times faster, respectively, than the terminal isomer 5HxO

211 (**1**). This dependence of reactivity on double bond location has implications for isoprene

212 hydroxyhydroperoxides (ISOPOOH) and hydroxynitrates (ISONO$_2$), which have both terminal

213 (β-) and non-terminal (δ-) isomers formed from gas-phase oxidation (Marais et al., 2016; Paulot

214 et al., 2009b; Paulot et al., 2009a). Based on our results we expect that the δ-isomers react more

215 quickly with organic triplets than the β-isomers.

216   Alkene stereochemistry also affects the triplet-alkene reaction rate constant. The data in

217 the middle of Fig. 2 shows that cis-HxO (**15**) reacts nearly five times more quickly with ^{3}BP*

218 than does trans-HxO (**10**), consistent with the lower predicted energy barrier for hydrogen atom

219 abstraction from the cis isomer. Finally, addition of electron-donating substituents (methyl

220 groups) on an unsaturated carbon atom also increases the rate constant. This is evident from

221 comparing 2B1O (**8**) and its methyl-substituted analog 3MBO (**12**): $k_{ALK+3BP*}$ is 3.7 times faster

222 with the methyl group (Fig. 2). Mechanistically, triplet-induced oxidation can proceed via either

223 hydrogen atom transfer or a proton-coupled-electron transfer (Canonica et al., 1995; Warren et

224 al., 2010; Erickson et al., 2015) and the presence of an electron-donating substituent on the

225 double bond likely selectively stabilizes the intermediates (e.g., radical or radical cation) formed

226 from these two processes, as well as the transition state structures for their formation.

227 **3.2 Relationship between *k* and one-electron oxidation potential**

228   Our next goal was to develop a quantitative structure-activity relationship (QSAR) so that

229 we can predict rate constants for alkene-triplet reactions. To use as predictor variables in the

230 QSARs we computed several properties of the alkenes: bond dissociation enthalpy and free

231 energy for various hydrogen atoms (Fig. S4), free energy and enthalpy barriers for hydrogen

232 atom abstraction (Table 1), and one-electron oxidation potentials (Table 1). Apart from the

233 oxidation potential, none of the other properties correlate well with the measured rate constants

234 (Figs. S5 and S6). While there is no correlation between the rate constants and predicted energy

235 barriers, alkenes with lower predicted free energy barriers ($\Delta G^{\ddagger}$) are predicted to be fast-reacting,

236 with rate constants above 5×10^8 M^{-1} s^{-1} (Fig. S6). As shown in Fig. S6, computed barriers

237 predict a much larger variation in rate than observed experimentally, suggesting that the breaking

238 of the C–H or O–H bond does not occur in the rate-determining step for all alkenes.

239   Of all the properties examined, the one-electron oxidation potential (OP) of the alkenes

240   best correlates with the (log of) measured rate constants, with rate constants generally increasing

241   as the alkenes are more easily oxidized, i.e., at lower OP values ($R^2 = 0.58$) (Fig. 3). Measured

242   rate constants for 13 of the 16 alkenes lie within (or very near to) the 95 % confidence interval

243   (blue lines) of the regression fit, but there are three notable outliers: hexen-1,3-diol (**3**, HDO),

244   cis-3-hexen-1-ol (**15**, cHxO) and cis-3-hexenylacetate (**16**, cHxAc). The measured HDO rate

245   constant is 3.3 times lower than that predicted by the regression line, while measured rate

246   constants for cHxO and cHxAc are 3.9 and 4.9 times higher, respectively, than predicted.

247   To try to assess why these compounds differ from the others, we calculated the highest

248   occupied molecular orbital (HOMO) of the alkene and the singly occupied molecular orbital

249   (SOMO) of the alkene radical cation (i.e., after oxidation) (Fig. 4). Depending on the system,

250   oxidation is predicted to occur by removing an electron either from the π system of the C–C

251   double bond or from a lone pair on the O atom. This is illustrated in Fig. 4, which shows the

252   HOMO and SOMO structures for HDO (**3**), where the electron is removed from the C-C double

253   bond, and 3B1O (**5**), where the electron is removed from the oxygen atom. However, the three

254   outliers in the correlation do not all fall into just one of these categories: for cHxAc (**16**) the

255   electron is most likely abstracted from the oxygen, while for HDO (**3**) and cHxO (**15**) the

256   electron is likely removed from the π system (Tables S2 and S3). This suggests that the location

257   of electron removal does not control the rate constants. We also examined if the rate of loss of

258   cHxO might be enhanced due to oligomerization, where an initially formed cHxO radical leads

259   to additional cHxO loss. Since the pseudo-first-order rate constant of oligomerization should

260   increase with initial cHxO concentration, we measured the rate constant for cHxO loss over a

261   range of initial concentrations (2–50 μM). However, as shown in Fig. S8, the rate constant for

262   cHxO loss does not depend on its concentration, suggesting that oligomerization is an

263   unimportant loss process for cHxO in our experiments. Thus, it is not clear why these three

264   compounds do not fall closer to the regression line of Fig. 3. However, except for **16**, all of the

265 alkenes fall within a factor of four of the correlation line (grey lines). Finally, even though there

266 is a good correlation between rate constant and OP in Fig. 3, it does not indicate whether these

267 reactions proceed via pure electron transfer, proton-coupled electron transfer, or hydrogen

268 transfer. As discussed earlier, since the predicted energy barriers for hydrogen abstraction do not

269 correlate with measured rate constants (Fig. S6) and appear to split into two groups, there

270 remains uncertainty about the mechanism of triplet-induced oxidation of the alkenes.

271 **3.3 Predicted triplet-OVOC bimolecular rate constants**

272   We next use the relationship in Fig. 3, along with calculated oxidation potentials, to

273 predict second-order rate constants for ^{3}BP* with a set of unsaturated <u>oxygenated VOCs formed</u>

274 <u>by the oxidation of</u> isoprene and limonene. As shown in Fig. 5, we predict that limonene

275 products generally react faster with ^{3}BP* than do isoprene products. For the five isoprene-

276 derived OVOCs that we considered, rate constants vary by a factor of 17, and range between

277 $(0.080–1.4) \times 10^9$ M^{-1} s^{-1} (Table 1, Fig. 5). The δ-isomers of ISOPOOH and ISONO$_2$, which

278 contain internal double bonds, have lower computed one-electron oxidation potentials and thus

279 higher predicted rate constants compared to the terminal β-isomers. This is similar to the trend

280 observed with the other alkenes (Fig. 2). In case of isoprene hydroperoxyaldehydes, we were

281 able to determine the oxidation potential for only HPALD2 (**22**), and its predicted reaction rate

282 constant (± 1 SE) of $4.0 (± 0.9) \times 10^8$ M^{-1} s^{-1} is among the lowest of the isoprene-derived alkenes

283 (Fig. 5).

284   We calculated OP values and triplet rate constants for three limonene-derived OVOCs:

285 limonene aldehyde (LMNALD) and two dihydroxy-limonene aldehydes (2,5OH-LMNALD and

286 4,7OH-LMNALD). Compared to the isoprene-derived alkenes, the rate constants for all three

287 limonene products are high, and range between $(0.89–1.7) \times 10^9$ M^{-1} s^{-1}. All of the limonene

288 aldehydes (as well as the isoprene products) can have several isomers whose calculated oxidation

289 potentials can vary, which affects the predicted rate constant. For example, for 4,7OH-LMNALD

290 (**25**) the computed oxidation potential for five of its isomers vary between 2.17 and 2.48 V

291 (Table S4), which leads to a relative standard deviation of 40 % in the predicted rate constants

292 for the various isomers. For each OVOC, the predicted rate constants in Table 1 are for the

293 lowest energy isomers whose structures are shown in Fig. S9.

294 **3.4 Role of triplets in the fate of isoprene- and limonene-derived OVOCs**

295   Next, we use our estimated rate constants, along with previously published estimated

296 values for rates of other loss processes (Table S5), to understand the importance of triplets as

297 sinks for isoprene- and limonene-derived OVOCs in a foggy/cloudy atmosphere. For our simple

298 calculations we use a liquid water content of 1×10^{-6} L-aq/L-g, a temperature of 25 °C, and

299 calculated Henry's law constants from EPISuite (US EPA. Estimation Programs Interface

300 Suite™ for Microsoft® Windows v 4.1, 2016) (Table S6). From these inputs, we estimate that

301 between 10 and 97 % of the OVOCs will be partitioned into the aqueous phase under our

302 conditions (Table S6). The OVOC sinks we consider are photolysis and reactions with hydroxyl

303 radical ($^{\bullet}OH$) and ozone (O_3) in the gas phase as well as hydrolysis and reactions with $^{\bullet}OH$, O_3,

304 and triplets in the aqueous phase (Table S5). Based on typical oxidant concentrations in both

305 phases and available rate constants with sinks, the overall pseudo-first-order rate constants for

306 <u>initial </u>OVOC loss<u>es</u> are estimated to be in the range of $(0.27–3.0) \times 10^{-4}$ s^{-1}, corresponding to

307 overall lifetimes of 0.93 to 10 h (Table S7). The only exception is δ-ISONO2, which is expected

308 to undergo rapid hydrolysis to form its corresponding diol (Jacobs et al., 2014) with a lifetime of

309 just 0.078 h (280 s).

310   Fig. 6 shows the overall loss rate constants, and the contribution from each pathway, for

311 four of these OVOCs: δ4-ISOPOOH (**19**), β-ISONO2 (**20**), HPALD2 (**22**) AND 4,7-OH

312 LMNALD (**25**). Overall, aqueous-phase processes dominate the fate of these OVOCs,

313 accounting for the bulk of their loss; but the contribution of aqueous triplets to OVOC loss

314 depends strongly on the triplet reactivity. Panel (a) of Fig. 6 shows OVOC loss when we assume

13

315 that the aqueous triplets are highly reactive, i.e., using rate constants estimated for [3]BP* (Fig. 5).

316 Since our recent measurements (Kaur et al., 2018; Kaur and Anastasio, 2018) indicate that, on

317 average, ambient triplets are not this reactive, this scenario likely represents an upper bound for

318 the triplet contribution. In this case highly reactive triplets are the dominant sinks for δ4-

319 ISOPOOH and 4,7-OH LMNALD, accounting for 74 % and 47 % of their total losses,

320 respectively (Fig. 6a). For β-ISONO$_2$ and HPALD2, triplets are not dominant but still significant,

321 accounting for 19 % and 24 % of loss, respectively, while other sinks dominate. For the OVOCs

322 where we calculated rate constants with [3]BP* (Fig. 5) but that are not shown in Fig. 6, the triplet

323 contribution varies widely, from less than 1 % for δ-ISONO2 (**21**), where hydrolysis dominates,

324 to 59 % for 2,5-OH LMNALD (**24**) (Table S7).

325   While [3]BP* likely represents an upper bound of triplet reactivity in atmospheric waters,

326 our recent measurements indicate that the triplets in fog waters and particles have an average

327 reactivity that is typically similar to 3'-methoxyacetophenone (3MAP) and 3,4-

328 dimethoxybenzaldehyde (DMB) (Kaur et al., 2018; Kaur and Anastasio, 2018). A comparison of

329 our [3]BP* rate constants (Table 1) with the average values for the 3MAP and DMB triplets for a

330 subset of the alkenes (Richards-Henderson et al., 2014b) indicates that the average 3MAP/DMB

331 triplet rate constants are 1–18 % of the corresponding [3]BP* values. Thus to scale alkene-triplet

332 rate constants from [3]BP* to the 3MAP and DMB triplets we take the median value of 4 %, which

333 is derived from the MeJA rate constants (Table S8). Fig. 6b shows the calculated fates of the

334 OVOCs in the case where we consider "typical reactivity" triplets, i.e., where we multiply the

335 [3]BP* + OVOC rate constants (Fig. 5) by a factor of 0.04. Under these conditions, triplets are

336 minor oxidants (Fig. 6b), accounting for 9 % and 3 % of the loss of δ4-ISOPOOH and 4,7-

337 LMNALD, respectively, and approximately 1 % for the other two OVOCs. This suggests that

338 aqueous triplets are generally minor sinks for OVOCs derived from isoprene and limonene, in

339 contrast to the case for phenols, where triplets appear to be the major sink (Smith et al., 2014; Yu

340 et al., 2014; Kaur and Anastasio, 2018). However, there are several important uncertainties in

341 our determination that triplets are likely minor sinks for oxygenated alkenes. First, the factor we

342 used to adjust from ^{3}BP* rate constants to triplet 3MAP/DMB rate constants (i.e., a factor of

343 0.04) is quite uncertain: values for the three BVOCs examined range from 0.01 to 0.18 (Table

344 S8). Additionally, there are very few measurements of triplets in atmospheric drops or particles

345 (Kaur et al., 2018; Kaur and Anastasio, 2018), and only from two sites, so it is possible that we

346 are underestimating the average reactivity and/or concentrations of triplets in atmospheric drops

347 and particles.

4   Conclusions

349   To explore whether triplet excited states of organic matter might be important sinks for

350 unsaturated organic compounds in atmospheric drops, we measured rate constants for 17 C_3–C_6

351 alkenes with the triplet excited state of benzophenone (^{3}BP*). The resulting bimolecular rate

352 constants span the range of (0.24–7.5) $\times$ 10^9 M^{-1}s^{-1}. Notably, the rate constants are high (above

353 10^9 M^{-1}s^{-1}) for some important green leaf volatiles emitted from plants – 3MBO, cHxO, cHxAc,

354 and MeJA. Rate constants appear to be enhanced by alkene characteristics such as an internal

355 double bond, cis-stereochemistry, and alkyl substitution on the double bond.

356   To be able to predict rate constants for other alkenes, we examined QSARs between our

357 measured rate constants and a variety of calculated properties for the alkenes and ^{3}BP*-alkene

358 transition states. Rate constants are not correlated with bond dissociation enthalpies, free

359 energies or predicted energy barriers for removal of various hydrogen atoms, but are reasonably

360 correlated with the one-electron oxidation potential of the alkenes ($R^2 = 0.58$). Based on the

361 relationship between rate constants and oxidation potential, we predict that highly reactive

362 triplets will react with first generation isoprene- and limonene- oxidation products with rate

363 constants on the order of 10^8–10^9 M^{-1} s^{-1}, with higher values for the δ–isomers compared to

364 terminal β–isomer products. Using these rate constants in a simple model of OVOC chemistry in

15

365 a foggy/cloudy atmosphere suggests that highly reactive aqueous triplets could be significant

366 oxidants for some isoprene hydroxyhydroperoxides and limonene aldehydes. However, for our

367 current best estimate of typical reactivities, triplets are a minor sink for isoprene- and limonene-

368 derived OVOCs.

369 To more specifically quantify the contributions of triplet excited states towards the loss of

370 alkenes in particles and drops requires more insight into both the reactivities and concentrations

371 of atmospheric triplet species. In addition, assessing whether triplets might be important sinks for

372 other organic species requires more measurements of reaction rate constants with

373 atmospherically relevant organics.

Competing Interests

375 The authors declare that they have no conflict of interest.

Author Contribution

377 CA and RK conceptualized the research goals and designed the experiments. RK and JD

378 performed the laboratory work, while BH and DT planned and performed the computational

379 calculations. RK analyzed the experimental data and prepared the manuscript with contributions

380 from all co-authors, particularly BH, who wrote the sections on computational calculations and

381 prepared the corresponding figures. CA reviewed and edited the manuscript. CA and DT

382 provided oversight during the entire process.

Data Availability

384 Data are available upon request.

Acknowledgements

16
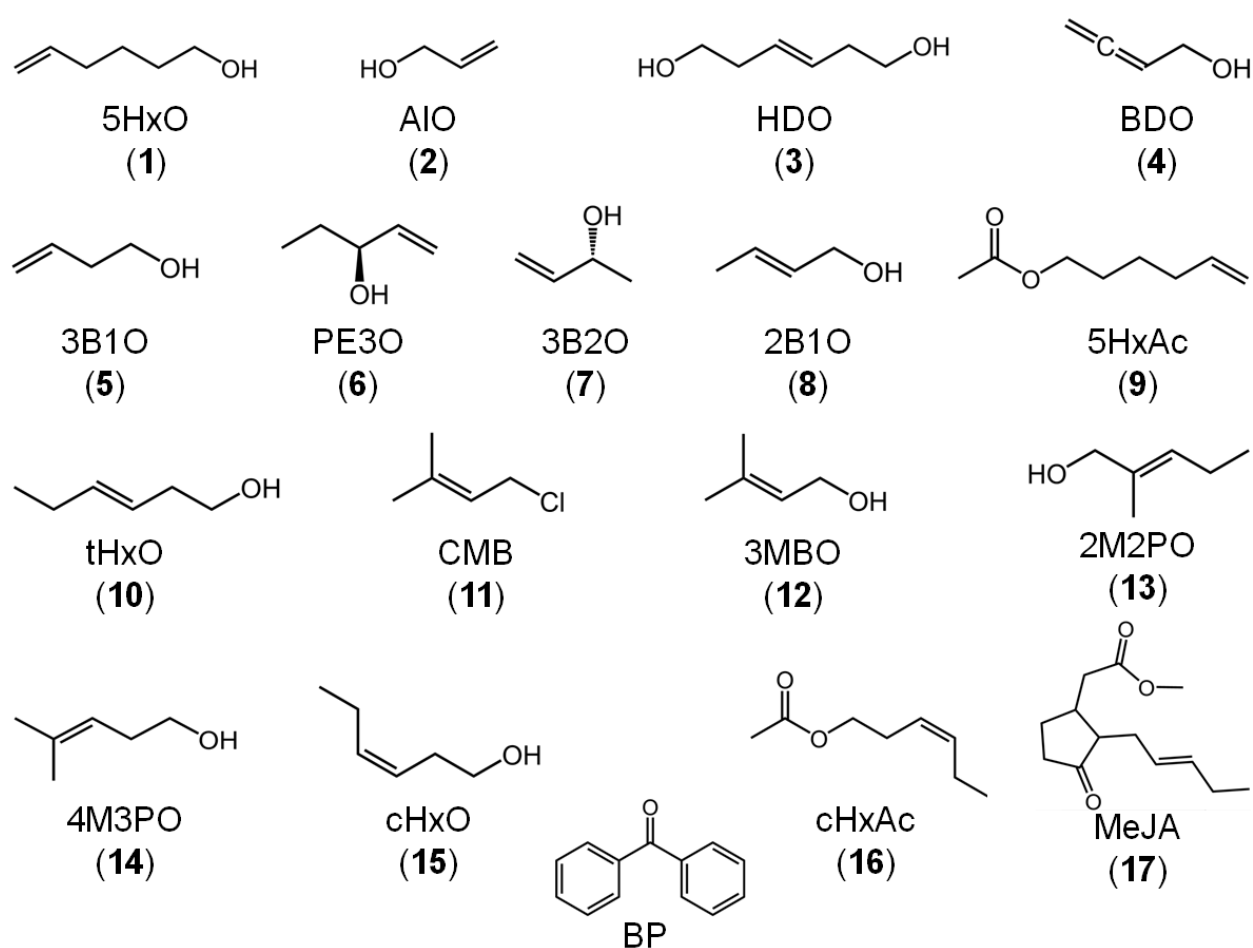
Fig. 1 Chemical structures of the reactant species used in this study: 17 alkenes and one model triplet, benzophenone. Compound numbers are in parentheses.
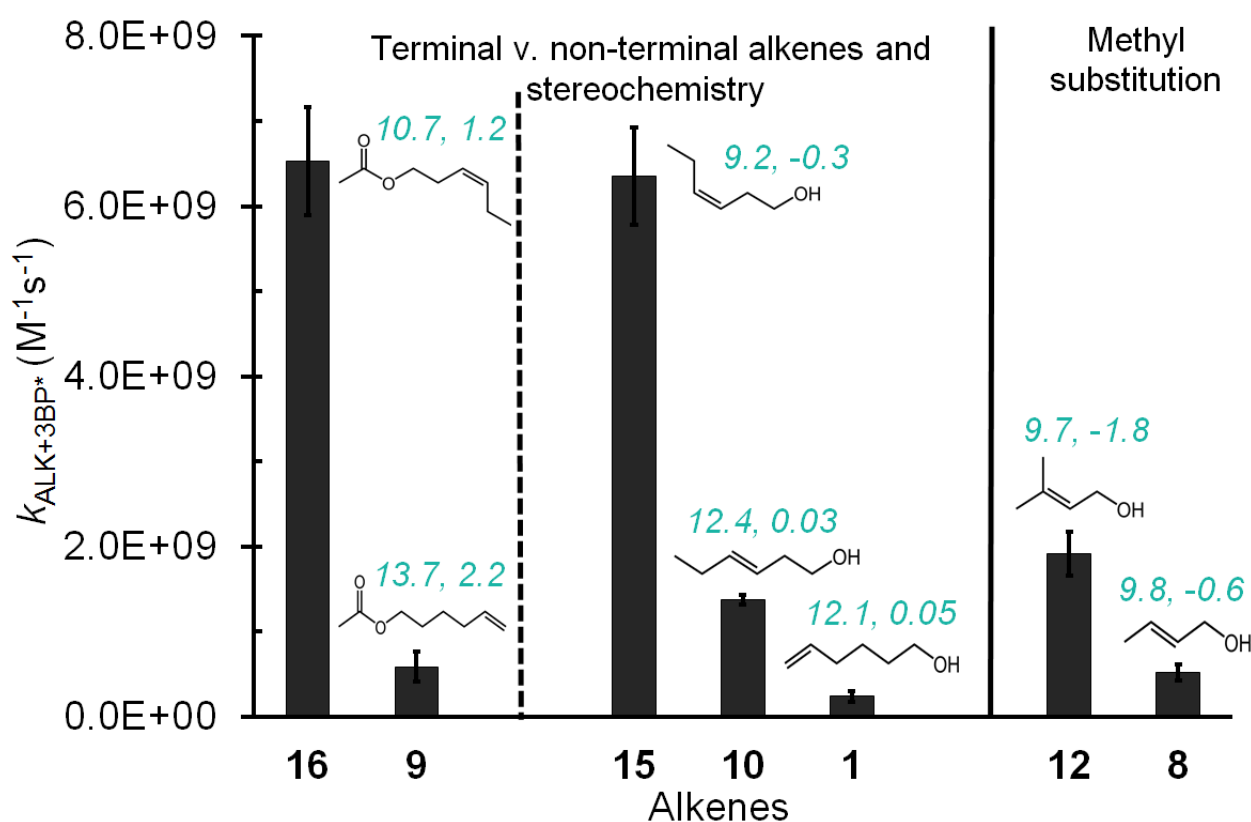
Fig. 2 Comparison of three sets of alkenes to illustrate how rate constants with the benzophenone triplet state vary with double bond location, stereochemistry, and methyl substitution. The teal numbers on each alkene represent the lowest free energy ($\Delta G^{\ddagger}$) and enthalpy ($\Delta H^{\ddagger}$) transition state barriers in kcal mol^{-1} for H-abstraction by triplet benzophenone; these were calculated at the uB3LYP/6-31+G(d,p) level of theory. Though computed barriers (Table 1) are not correlated with the overall rates measured, they broadly match the rate trends within a given set of alkenes in this figure.

404
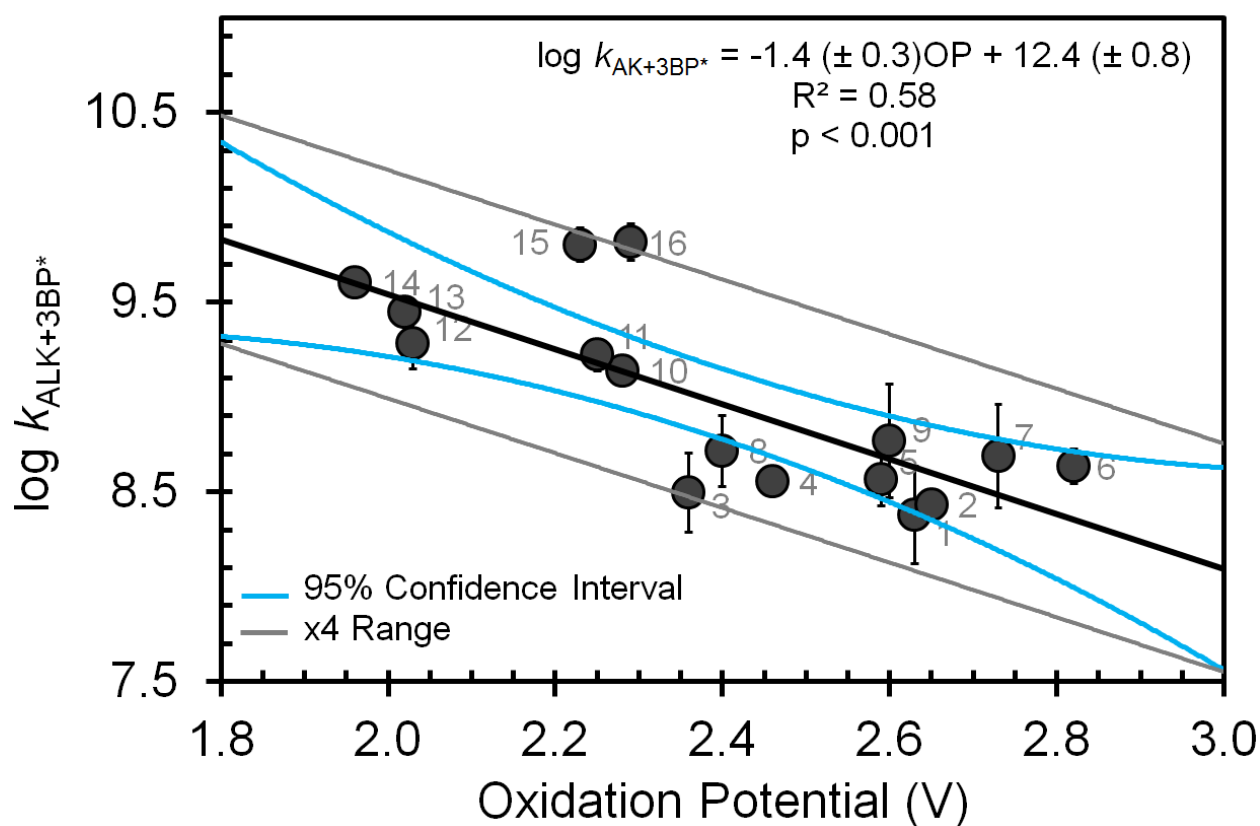
Fig. 3 Correlation between measured bimolecular rate constants for alkenes with the triplet excited state of benzophenone ($k_{ALK+3BP*}$) and the computed one-electron oxidation potentials of the alkenes. Numbers on each point represent the alkene numbers in Table 1. Blue lines represent 95 % confidence intervals of the regression prediction. The gray lines bound the region that is within a factor of four of the regression prediction; all but one of the alkene values fall within this. Methyl jasmonate (**17**) is not included in this figure due to computational challenges in calculating its OP (see Table 1).

a) Electron removed from the π system

HDO
(3)

105.4
(100.3)   HO

85.7
(78.5)

95.5
(98.3)   OH

HOMO

SOMO

1.20

1.46

$\Delta G^{\ddagger} = 12.3$ kcal/mol
$\Delta H^{\ddagger} = 0.2$ kcal/mol

b) Electron removed from the oxygen

3B1O
(5)

94.1
(88.1)

84.4
(76.9)   OH

105.4
(100.5)

HOMO

SOMO

1.20

1.45

$\Delta G^{\ddagger} = 9.8$ kcal/mol
$\Delta H^{\ddagger} = -1.2$ kcal/mol
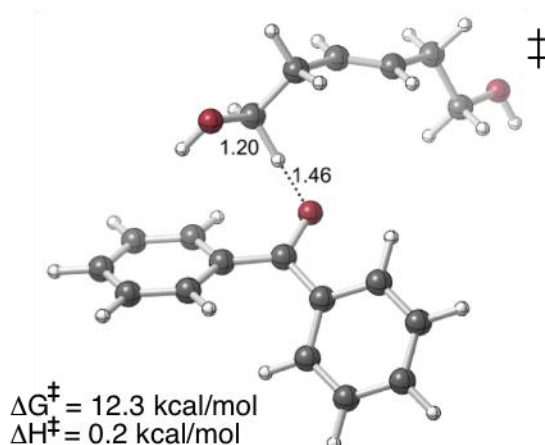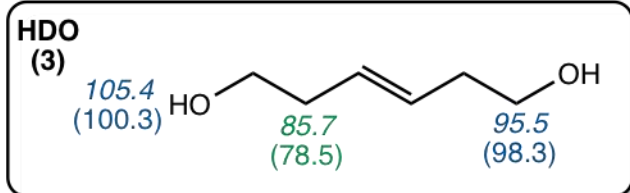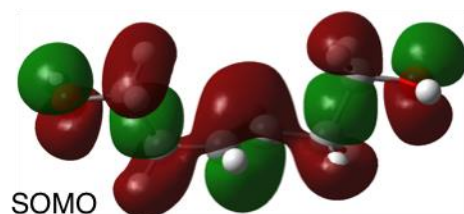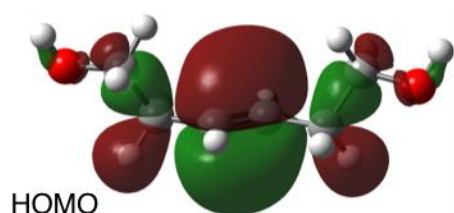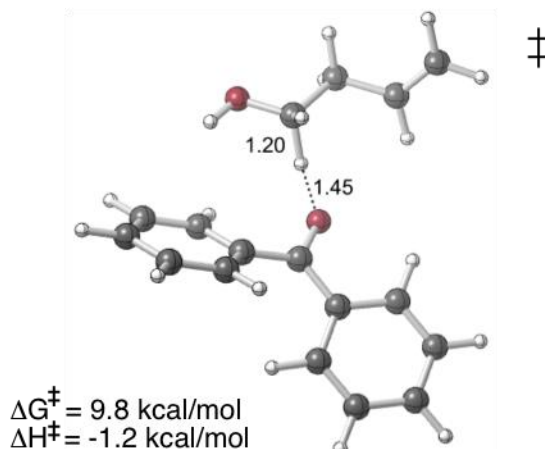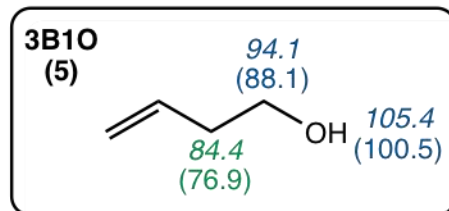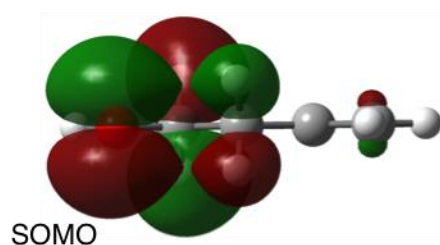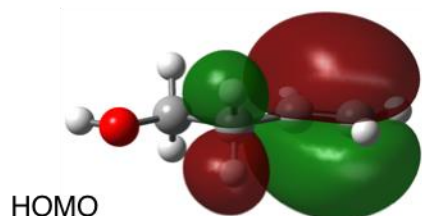
Fig. 4 Diagrams of the highest occupied molecular orbitals (HOMOs) of the alkenes before oxidation, and the singly occupied molecular orbitals (SOMOs) after removal of one electron from the alkenes, and lowest energy transition state structures (‡) of alkenes **3** and **5**. Bond dissociation enthalpy (italicized) and free energy (in parentheses) for various hydrogen atoms (in kcal mol^{-1}) for each alkene are shown in the boxes. Numbers in green are the lowest values, and thus represent the most labile hydrogen in each alkene. *a)* The electron removed during H-abstraction of HDO is predicted to come from the π system, but this results in delocalization due to hyperconjugation. *b)* The electron removed from 3B1O during H-abstraction is predicted to come from the oxygen. See SI Tables S2 and S3 for HOMO/SOMO structures and Fig. S4 for the bond dissociation enthalpies and free energies for other alkenes.

21
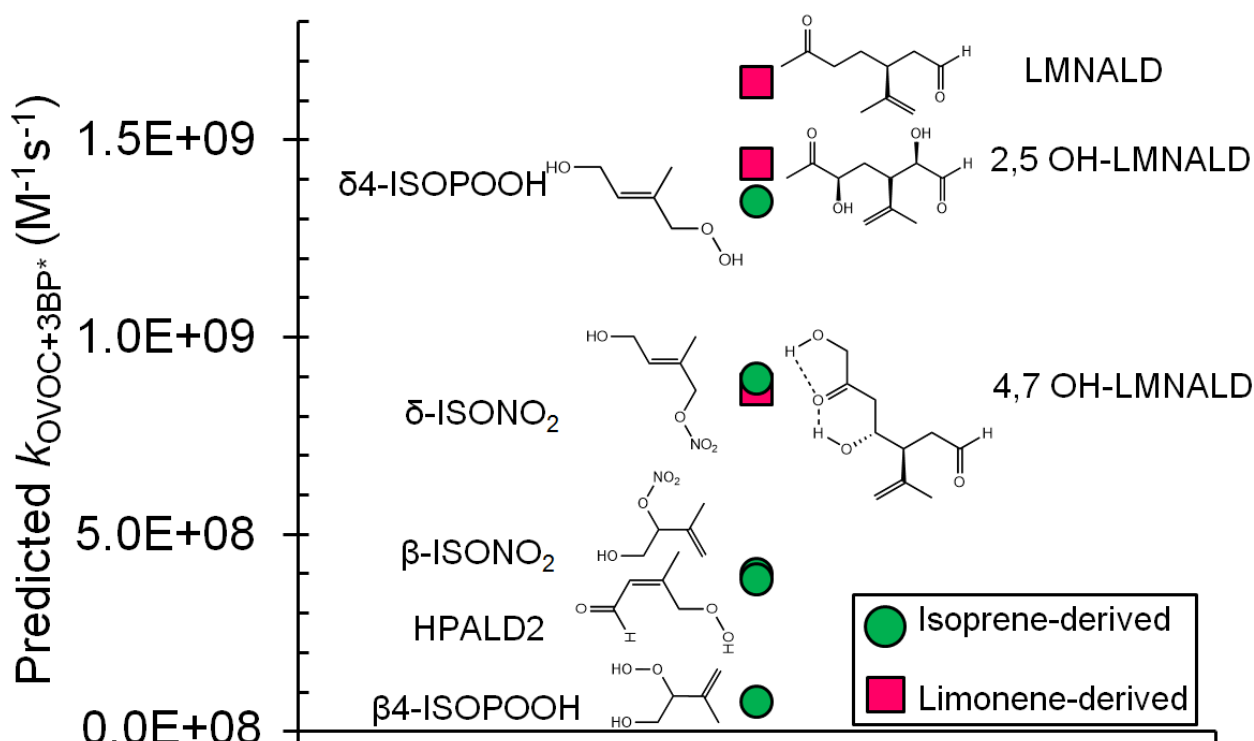
Fig. 5 Predicted bimolecular rate constants for a range of limonene and isoprene oxidation products (OVOCs) with the triplet state of BP. Rate constants are estimated from the QSAR with one-electron oxidation potentials (OPs) (Fig. 3). Oxidation potentials used to predict the rate constants here (and in Table 1) are for the lowest energy isomers of the OVOCs, which are the structures shown here. The structures of some of the other, higher energy, isomers are shown in Table S4.
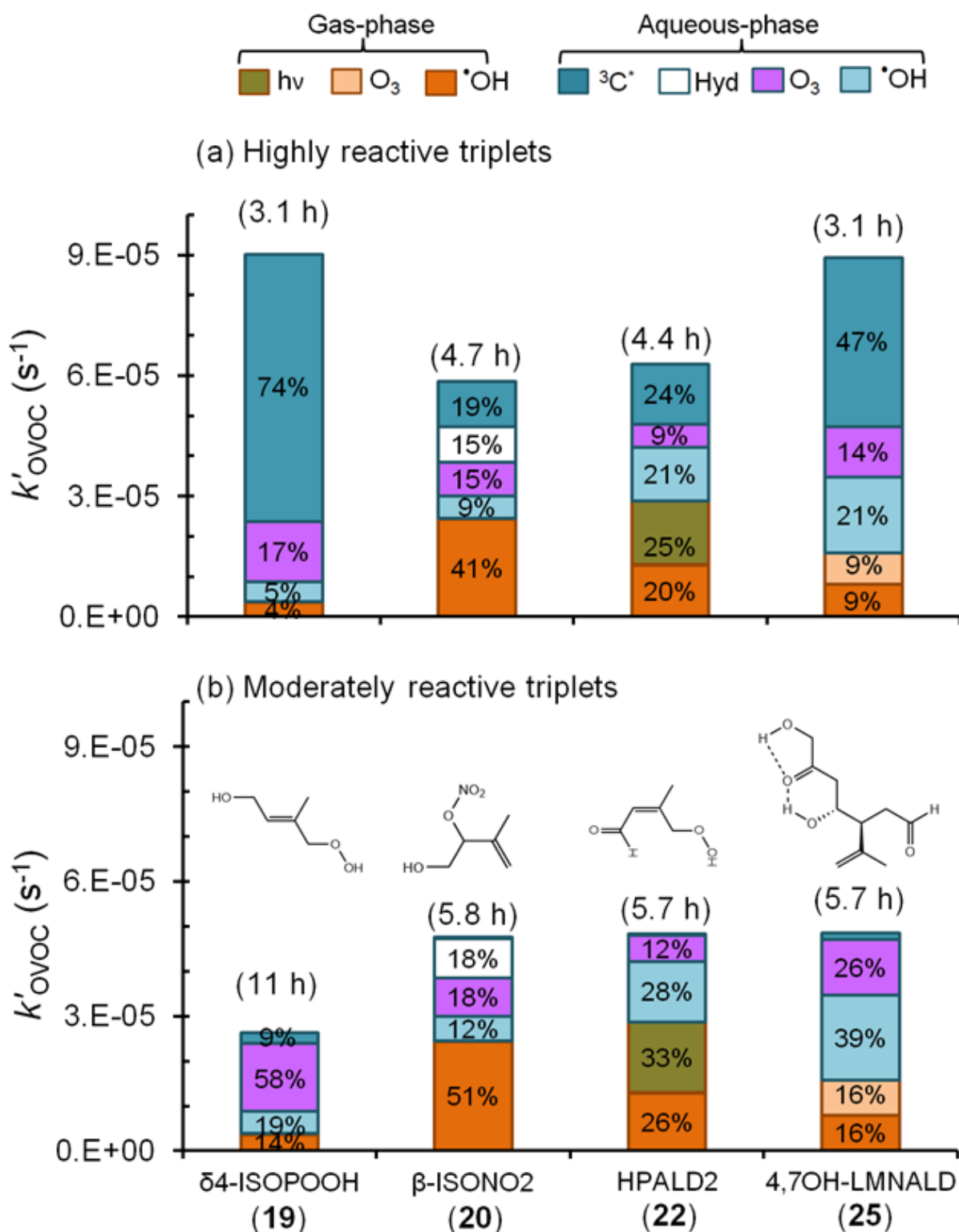
Fig. 6 Estimated pseudo-first-order loss rate constants and corresponding lifetimes (in parentheses) for representative isoprene- and limonene-derived oxidation products in a foggy atmosphere (Tables S5–S7). Colors and data labels indicate the percentage of OVOC lost via each gas and aqueous pathway, including direct photoreaction (hν) and hydrolysis (Hyd); pathways contributing less than 4 % are not labeled. Panel (a) is a likely upper bound for the triplet contributions to OVOC loss where we assume that all fog triplets are highly reactive, like benzophenone. Panel (b) shows the more likely contribution from triplets, assuming moderately reactive triplets that are more representative of the average measured in fog waters and aqueous particle extracts(Kaur et al., 2018; Kaur and Anastasio, 2018) (Tables S5–S7).

442   **References**

443   Anastasio, C., Faust, B. C., and Allen, J. M.: Aqueous-phase photochemical formation of
444   hydrogen peroxide in authentic cloud waters, J. Geophys. Res. Atmos., 99, 8231-8248,
445   1994.
446   Anastasio, C., Faust, B. C., and Rao, C. J.: Aromatic carbonyl compounds as aqueous-phase
447   photochemical sources of hydrogen peroxide in acidic sulfate aerosols, fogs, and clouds.
448   1. Non-phenolic methoxybenzaldehydes and methoxyacetophenones with reductants
449   (phenols), Environmental science & technology, 31, 218-232, 1996.
450   Anastasio, C., and McGregor, K. G.: Chemistry of fog waters in California's central valley: 1. In
451   situ photoformation of hydroxyl radical and singlet molecular oxygen, Atmos. Environ.,
452   35, 1079-1089, 2001.
453   Arnold, W. A.: One electron oxidation potential as a predictor of rate constants of N-containing
454   compounds with carbonate radical and triplet excited state organic matter, Environ. Sci.
455   Process. Impact., 16, 832-838, 2014.
456   Bahnmüller, S., von Gunten, U., and Canonica, S.: Sunlight-induced transformation of
457   sulfadiazine and sulfamethoxazole in surface waters and wastewater effluents, Water
458   Res., 57, 183-192, 2014.
459   Becke, A. D.: Density-functional thermochemistry. I. The effect of the exchange-only gradient
460   correction, The Journal of chemical physics, 96, 2155-2160, 1992.
461   Becke, A. D.: Becke's three parameter hybrid method using the LYP correlation functional, J.
462   Chem. Phys, 98, 5648-5652, 1993.
463   Blando, J. D., and Turpin, B. J.: Secondary organic aerosol formation in cloud and fog droplets:
464   A literature evaluation of plausibility, Atmos. Environ., 34, 1623-1632, 2000.
465   Boreen, A. L., Arnold, W. A., and McNeill, K.: Triplet-sensitized photodegradation of sulfa
466   drugs containing six-membered heterocyclic groups: identification of an SO2 extrusion
467   photoproduct, Environmental science & technology, 39, 3630-3638, 2005.
468   Canonica, S., and Hoigné, J.: Enhanced oxidation of methoxy phenols at micromolar
469   concentration photosensitized by dissolved natural organic material, Chemosphere, 30,
470   2365-2374, 1995.
471   Canonica, S., Jans, U., Stemmler, K., and Hoigne, J.: Transformation kinetics of phenols in
472   water: Photosensitization by dissolved natural organic material and aromatic ketones,
473   Environ. Sci. Technol., 29, 1822-1831, 1995.
474   Canonica, S., Hellrung, B., and Wirz, J.: Oxidation of phenols by triplet aromatic ketones in
475   aqueous solution, J. Phys. Chem. A, 104, 1226-1232, 2000.
476   Canonica, S., Hellrung, B., Müller, P., and Wirz, J.: Aqueous oxidation of phenylurea herbicides
477   by triplet aromatic ketones, Environ. Sci. Technol., 40, 6636-6641, 2006a.
478   Canonica, S., Hellrung, B., Müller, P., and Wirz, J.: Aqueous oxidation of phenylurea herbicides
479   by triplet aromatic ketones, Environmental science & technology, 40, 6636-6641, 2006b.
480   Crounse, J. D., Paulot, F., Kjaergaard, H. G., and Wennberg, P. O.: Peroxy radical isomerization
481   in the oxidation of isoprene, Phys. Chem. Chem. Phys., 13, 13607-13613, 2011.
482   Erickson, P. R., Walpen, N., Guerard, J. J., Eustis, S. N., Arey, J. S., and McNeill, K.:
483   Controlling factors in the rates of oxidation of anilines and phenols by triplet methylene
484   blue in aqueous solution, J. Phys. Chem. A, 119, 3233-3243, 2015.
485   Finlayson-Pitts, B. J., and Pitts Jr, J. N.: Chemistry of the Upper and Lower Atmosphere:
486   Theory, Experiments, and Applications, Academic press, 1999.
487   Frisch, M., Trucks, G., Schlegel, H. B., Scuseria, G., Robb, M., Cheeseman, J., Scalmani, G.,
488   Barone, V., Mennucci, B., and Petersson, G.: Gaussian 09, revision a. 02, gaussian, Inc.,
489   Wallingford, CT, 200, 2009.

490   Fu, H., Ciuraru, R., Dupart, Y., Passananti, M., Tinel, L., Rossignol, S. p., Perrier, S., Donaldson,
491   D. J., Chen, J., and George, C.: Photosensitized production of atmospherically reactive
492   organic compounds at the air/aqueous interface, J. Am. Chem. Soc., 137, 8348-8351,
493   2015.
494   Gelencsér, A., and Varga, Z.: Evaluation of the atmospheric significance of multiphase reactions
495   in atmospheric secondary organic aerosol formation, Atmos. Chem. Phys., 5, 2823-2831,
496   2005.
497   Hallquist, M., Wenger, J., Baltensperger, U., Rudich, Y., Simpson, D., Claeys, M., Dommen, J.,
498   Donahue, N., George, C., and Goldstein, A.: The formation, properties and impact of
499   secondary organic aerosol: current and emerging issues, Atmos. Chem. Phys., 9, 5155-
500   5236, 2009.
501   Herrmann, H., Hoffmann, D., Schaefer, T., Bräuer, P., and Tilgner, A.: Tropospheric aqueous-
502   phase free-radical chemistry: Radical sources, spectra, reaction kinetics and prediction
503   tools, ChemPhysChem, 11, 3796-3822, 2010.
504   Herrmann, H., Schaefer, T., Tilgner, A., Styler, S. A., Weller, C., Teich, M., and Otto, T.:
505   Tropospheric aqueous-phase chemistry: Kinetics, mechanisms, and its coupling to a
506   changing gas phase, Chem. Rev., 115, 4259-4334, 2015.
507   Jacobs, M. I., Burke, W., and Elrod, M. J.: Kinetics of the reactions of isoprene-derived
508   hydroxynitrates: gas phase epoxide formation and solution phase hydrolysis, Atmos.
509   Chem. Phys., 14, 8933-8946, 2014.
510   Kaur, R., and Anastasio, C.: Light absorption and the photoformation of hydroxyl radical and
511   singlet oxygen in fog waters, Atmos. Environ., 164, 387-397, 2017.
512   Kaur, R., and Anastasio, C.: First Measurements of Organic Triplet Excited States in
513   Atmospheric Waters, Environ. Sci. Technol., 52, 5218-5226, 2018.
514   Kaur, R., Labins, J. R., Helbock, S. S., Jiang, W., K.J., B., Zhang, Q., and Anastasio, C.:
515   Photooxidants from Brown Carbon and Other Chromophores in Illuminated Particle
516   Extracts, *In Preparation*, 2018.
517   Khamaganov, V. G., and Hites, R. A.: Rate Constants for the Gas-Phase Reactions of Ozone
518   with Isoprene, α-and β-Pinene, and Limonene as a Function of Temperature, The Journal
519   of Physical Chemistry A, 105, 815-822, 2001.
520   Kroll, J. H., and Seinfeld, J. H.: Chemistry of secondary organic aerosol: Formation and
521   evolution of low-volatility organics in the atmosphere, Atmos. Environ., 42, 3593-3624,
522   2008.
523   Laskin, A., Laskin, J., and Nizkorodov, S. A.: Chemistry of atmospheric brown carbon, Chem.
524   Rev., 115, 4335-4382, 2015.
525   Lee, A. K., Herckes, P., Leaitch, W., Macdonald, A., and Abbatt, J.: Aqueous OH oxidation of
526   ambient organic aerosol and cloud water organics: Formation of highly oxidized
527   products, Geophys. Res. Lett., 38, 2011.
528   Lee, C., Yang, W., and Parr, R. G.: Development of the Colle-Salvetti correlation-energy
529   formula into a functional of the electron density, Physical review B, 37, 785, 1988.
530   Lee, L., Teng, A. P., Wennberg, P. O., Crounse, J. D., and Cohen, R. C.: On Rates and
531   Mechanisms of OH and O_3 Reactions with Isoprene-Derived Hydroxy Nitrates, The
532   Journal of Physical Chemistry A, 118, 1622-1637, 2014.
533   Legault, C.: CYLview, 1.0 b, Université de Sherbrooke, 2009.
534   Li, W.-Y., Li, X., Jockusch, S., Wang, H., Xu, B., Wu, Y., Tsui, W. G., Dai, H.-L., McNeill, V.
535   F., and Rao, Y.: Photoactivated production of secondary organic species from isoprene in
536   aqueous systems, The Journal of Physical Chemistry A, 120, 9042-9048, 2016.

Lim, Y., Tan, Y., Perri, M., Seitzinger, S., and Turpin, B.: Aqueous chemistry and its role in secondary organic aerosol (SOA) formation, Atmos. Chem. Phys., 10, 10521-10539, 2010.

Marais, E. A., Jacob, D. J., Jimenez, J. L., Campuzano-Jost, P., Day, D. A., Hu, W., Krechmer, J., Zhu, L., Kim, P. S., and Miller, C. C.: Aqueous-phase mechanism for secondary organic aerosol formation from isoprene: application to the southeast United States and co-benefit of SO 2 emission controls, Atmos. Chem. Phys., 16, 1603-1618, 2016.

Marenich, A. V., Cramer, C. J., and Truhlar, D. G.: Universal solvation model based on the generalized Born approximation with asymmetric descreening, Journal of chemical theory and computation, 5, 2447-2464, 2009.

Mayer, P. M., Parkinson, C. J., Smith, D. M., and Radom, L.: An assessment of theoretical procedures for the calculation of reliable free radical thermochemistry: A recommended new procedure, The Journal of chemical physics, 108, 604-615, 1998.

McNeill, K., and Canonica, S.: Triplet state dissolved organic matter in aquatic photochemistry: Reaction mechanisms, substrate scope, and photophysical properties, Environ. Sci. Process. Impact., 18, 1381-1399, 2016.

Montgomery Jr, J. A., Frisch, M. J., Ochterski, J. W., and Petersson, G. A.: A complete basis set model chemistry. VI. Use of density functional geometries and frequencies, The Journal of chemical physics, 110, 2822-2827, 1999.

Ng, N., Kwan, A., Surratt, J., Chan, A., Chhabra, P., Sorooshian, A., Pye, H. O., Crounse, J., Wennberg, P., and Flagan, R.: Secondary organic aerosol (SOA) formation from reaction of isoprene with nitrate radicals (NO 3), Atmos. Chem. Phys., 8, 4117-4140, 2008.

Paulot, F., Crounse, J., Kjaergaard, H., Kroll, J., Seinfeld, J., and Wennberg, P.: Isoprene photooxidation: new insights into the production of acids and organic nitrates, Atmos. Chem. Phys., 9, 1479-1501, 2009a.

Paulot, F., Crounse, J. D., Kjaergaard, H. G., Kürten, A., Clair, J. M. S., Seinfeld, J. H., and Wennberg, P. O.: Unexpected epoxide formation in the gas-phase photooxidation of isoprene, Science, 325, 730-733, 2009b.

Petersson, a., Bennett, A., Tensfeldt, T. G., Al-Laham, M. A., Shirley, W. A., and Mantzaris, J.: A complete basis set model chemistry. I. The total energies of closed-shell atoms and hydrides of the first-row elements, The Journal of chemical physics, 89, 2193-2218, 1988.

Petersson, G., and Al-Laham, M. A.: A complete basis set model chemistry. II. Open-shell systems and the total energies of the first-row atoms, The Journal of chemical physics, 94, 6081-6090, 1991.

Petersson, G., Tensfeldt, T. G., and Montgomery Jr, J.: A complete basis set model chemistry. III. The complete basis set-quadratic configuration interaction family of methods, The Journal of chemical physics, 94, 6091-6101, 1991.

Richards-Henderson, N. K., Pham, A. T., Kirk, B. B., and Anastasio, C.: Secondary Organic Aerosol from Aqueous Reactions of Green Leaf Volatiles with Organic Triplet Excited States and Singlet Molecular Oxygen, Environmental Science & Technology, 49, 268-276, 2014a.

Richards-Henderson, N. K., Pham, A. T., Kirk, B. B., and Anastasio, C.: Secondary organic aerosol from aqueous reactions of green leaf volatiles with organic triplet excited states and singlet molecular oxygen, Environ. Sci. Technol., 49, 268-276, 2014b.

Rossignol, S. p., Aregahegn, K. Z., Tinel, L., Fine, L., Nozière, B., and George, C.: Glyoxal induced atmospheric photosensitized chemistry leading to organic aerosol growth, Environmental science & technology, 48, 3218-3227, 2014.

Schöne, L., and Herrmann, H.: Kinetic measurements of the reactivity of hydrogen peroxide and ozone towards small atmospherically relevant aldehydes, ketones and organic acids in aqueous solutions, Atmos. Chem. Phys., 14, 4503, 2014.

Smith, J. D., Sio, V., Yu, L., Zhang, Q., and Anastasio, C.: Secondary organic aerosol production from aqueous reactions of atmospheric phenols with an organic triplet excited state, Environ. Sci. Technol., 48, 1049-1057, 2014.

St. Clair, J. M., Rivera-Rios, J. C., Crounse, J. D., Knap, H. C., Bates, K. H., Teng, A. P., Jørgensen, S., Kjaergaard, H. G., Keutsch, F. N., and Wennberg, P. O.: Kinetics and Products of the Reaction of the First-Generation Isoprene Hydroxy Hydroperoxide (ISOPOOH) with OH, The Journal of Physical Chemistry A, 120, 1441-1451, 2015.

Stephens, P., Devlin, F., Chabalowski, C., and Frisch, M. J.: Ab initio calculation of vibrational absorption and circular dichroism spectra using density functional force fields, J. Phys. Chem., 98, 11623-11627, 1994.

Surratt, J. D., Murphy, S. M., Kroll, J. H., Ng, N. L., Hildebrandt, L., Sorooshian, A., Szmigielski, R., Vermeylen, R., Maenhaut, W., and Claeys, M.: Chemical composition of secondary organic aerosol formed from the photooxidation of isoprene, The Journal of Physical Chemistry A, 110, 9665-9690, 2006.

Tirado-Rives, J., and Jorgensen, W. L.: Performance of B3LYP density functional methods for a large set of organic molecules, Journal of Chemical Theory and Computation, 4, 297-306, 2008.

Tsui, W. G., Rao, Y., Dai, H.-L., and McNeill, V. F.: Modeling photosensitized secondary organic aerosol formation in laboratory and ambient aerosols, Environ. Sci. Technol., 51, 7496-7501, 2017.

US EPA. Estimation Programs Interface Suite™ for Microsoft® Windows v 4.1: Estimation Programs Interface Suite™ for Microsoft® Windows, v 4.1. United States Environmental Protection Agency, Washington, DC, USA., 2016.

Volkamer, R., Ziemann, P., and Molina, M.: Secondary organic aerosol formation from acetylene (C 2 H 2): seed effect on SOA yields due to organic photochemistry in the aerosol aqueous phase, Atmos. Chem. Phys., 9, 1907-1928, 2009.

Walser, M. L., Desyaterik, Y., Laskin, J., Laskin, A., and Nizkorodov, S. A.: High-resolution mass spectrometric analysis of secondary organic aerosol produced by ozonation of limonene, Phys. Chem. Chem. Phys., 10, 1009-1022, 2008.

Warren, J. J., Tronic, T. A., and Mayer, J. M.: Thermochemistry of proton-coupled electron transfer reagents and its implications, Chem. Rev., 110, 6961-7001, 2010.

Wilkinson, F., Helman, W. P., and Ross, A. B.: Rate constants for the decay and reactions of the lowest electronically excited singlet-state of molecular-oxygen in solution - an expanded and revised compilation, J. Phys. Chem. Ref. Data, 24, 663-1021, 1995.

Wolfe, G. M., Crounse, J. D., Parrish, J. D., Clair, J. M. S., Beaver, M. R., Paulot, F., Yoon, T. P., Wennberg, P. O., and Keutsch, F. N.: Photolysis, OH Reactivity and Ozone Reactivity of a Proxy for Isoprene-Derived Hydroperoxyenals (HPALDs), Phys. Chem. Chem. Phys., 14, 7276-7286, 2012.

Yu, L., Smith, J., Laskin, A., Anastasio, C., Laskin, J., and Zhang, Q.: Chemical characterization of SOA formed from aqueous-phase reactions of phenols with the triplet excited state of carbonyl and hydroxyl radical, Atmos. Chem. Phys., 14, 13801-13816, 2014.

Zepp, R. G., Wolfe, N. L., Baughman, G. L., and Hollis, R. C.: Singlet oxygen in natural waters, Nature, 267, 421-423, 1977.

Zhang, Q., Jimenez, J. L., Canagaratna, M. R., Allan, J. D., Coe, H., Ulbrich, I., Alfarra, M. R., Takami, A., Middlebrook, A. M., Sun, Y. L., Dzepina, K., Dunlea, E., Docherty, K.,

633   DeCarlo, P. F., Salcedo, D., Onasch, T., Jayne, J. T., Miyoshi, T., Shimono, A.,
634   Hatakeyama, S., Takegawa, N., Kondo, Y., Schneider, J., Drewnick, F., Borrmann, S.,
635   Weimer, S., Demerjian, K., Williams, P., Bower, K., Bahreini, R., Cottrell, L., Griffin, R.
636   J., Rautiainen, J., Sun, J. Y., Zhang, Y. M., and Worsnop, D. R.: Ubiquity and dominance
637   of oxygenated species in organic aerosols in anthropogenically-influenced northern
638   hemisphere midlatitudes, Geophys. Res. Lett., 34, n/a-n/a, 2007.

639

640 **Table 1.** Measured alkene-benzophenone triplet reaction rate constants, predicted OVOC-
641 benzophenone triplet reaction rate constants, and computed parameters for the alkenes.

#	Name	Abbreviation	OP [a] (V)	$\Delta G^{\ddagger}$ [b] (kcal mol^{-1})	$\Delta H^{\ddagger}$ [c] (kcal mol^{-1})	Measured $k_{ALK+3BP*}$ [d] (10^8 M^{-1}s^{-1})
Alkenes						
1	5-Hexen-1-ol	5HxO	2.63	12.1	0.05	2.4 (0.6)
2	2-Propen-1-ol (Allyl alcohol)	AlO	2.65	10.8	-0.04	2.7 (0.2)
3	3-Hexene-1,6-diol	HDO	2.36	12.3	0.2	3.1 (0.7)
4	2,3-Butadien-1-ol	BDO	2.46	10.5	-1.5	3.6 (0.3)
5	3-Buten-1-ol	3B1O	2.59	9.8	-1.2	3.7 (0.5)
6	1-Penten-3-ol	PE3O	2.82	11.3	-1.0	4.3 (0.4)
7	3-Buten-2-ol	3B2O	2.73	10.6	-1.0	4.9 (1.3)
8	2-Buten-1-ol	2B1O	2.40	9.8	-0.6	5.2 (1.0)
9	5-Hexenyl acetate	5HxAc	2.60	13.7	2.2	5.9 (1.8)
10	trans-3-hexen-1-ol	tHxO	2.28	12.4	0.03	14 (1)
11	1-Chloro-3-methyl-2-butene	CMB	2.25	14.1	2.7	17 (1) [e]
12	3-Methyl-2-buten-1-ol (Prenol)	3MBO	2.03	9.7	-1.8	19 (3)
13	2-Methyl-2-penten-1-ol	2M2PO	2.02	11.6	-1.4	28 (1)
14	4-Methyl-3-penten-1-ol	4M3PO	1.96	11.5	-0.4	40 (2)
15	cis-3-Hexen-1-ol	cHxO	2.23	9.2	-0.3	64 (6)
16	cis-3-Hexenyl acetate	cHxAc	2.29	10.7	1.2	65 (6)
17	Methyl jasmonate	MeJA	- [f]	- [f]	- [f]	75 (5)
Predictions for isoprene- and limonene-derived OVOCs						Predicted $k_{OVOC+3BP*}$ [g] (10^8 M^{-1}s^{-1})
18	β4-Isoprene hydroxyhydroperoxide	β4-ISOPOOH	3.13	13.2	0.3	0.80 (0.18)
19	δ4-Isoprene hydroxyhydroperoxide	δ4-ISOPOOH	2.28	10.5	-2.0	14 (3)
20	β-Isoprene hydroxynitrate	β-ISONO2	2.64	13.2	1.4	4.1 (0.9)
21	δ-Isoprene hydroxynitrate	δ-ISONO2	2.40	10.0	-1.9	9.2 (2.1)
22	Isoprene hydroperoxyaldehyde 2	HPALD2	2.65	10.4	-2.6	4.0 (0.9)
23	Limononaldehdye	LMNALD	2.22	9.9	-1.4	17 (4)
24	2,5-Dihydroxy limononaldehdye	2,5OH-LMNALD	2.26	10.1	-2.2	15 (3)
25	4,7-Dihydroxy limononaldehdye	4,7-OH-LMNALD	2.41	10.6	-0.8	8.9 (2.0)

642   [a] One-electron oxidation potential, calculated using the CBS-QB3 compound method.
643   [b,c] Lowest transition state energy barrier for H-abstraction by triplet benzophenone, calculated using
644   uB3LYP/6-31+G(d,p).
645   [d] Measured bimolecular rate constant for alkene reacting with ^{3}BP* with uncertainties of ± 1 standard
646   deviation, determined from triplicate measurements (Table S1 of the supplement).

647   [e] Listed uncertainty is ± 1 standard error, n =1.

648   [f] The oxidation potential and energy barriers could not be computed for MeJA (**17**). Because the CB3-

649   QB3 method scales at N^7 (where N is the number of atoms), the larger compound required more

650   computational power than available.

651   [g] Predicted bimolecular rate constant for select isoprene- and limonene-derived OVOCs reacting with

652        $^3BP^*$, determined from the correlation between OP and $k_{ALK+3BP^*}$. Listed uncertainties are ± 1 standard

653   error propagated from the error of the slope of the quantitative structure-activity relationship between

654   oxidation potential and $k_{ALK+3BP^*}$ (Fig. 3).

1   Supporting Information for:

2

3   **Aqueous Reactions of Organic Triplet Excited States with Atmospheric**
4   **Alkenes**

5   Richie Kaur [a], Brandi M. Hudson [b], Joseph Draper [a, #], Dean J. Tantillo [b], and Cort Anastasio [*a]

6   [a] Department of Land, Air, and Water Resources, University of California, Davis, California
7   95616, United States

8   [b] Department of Chemistry, University of California, Davis, California 95616, United States

9   [#] Now at the Fresno Metropolitan Flood Control District, California 93727, United States

10

11   Correspondence to: C. Anastasio (canastasio@ucdavis.edu)

12

13   This supporting information contains: 19 Pages, 8 Tables, and 9 Figures

14

16

Table S1. Reference probes and triplicate measurements of rate constants for alkenes in a solution at pH 5.5. Errors (in parentheses) for each replicate measurement represent ± 1 standard error, determined by propagating errors in the slope of the relative rate plot and in the reference compound rate constant. Errors on the average values represent ± 1 σ determined from the average of the replicate values.
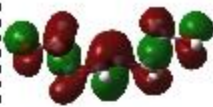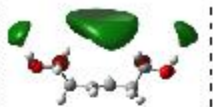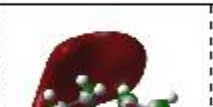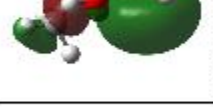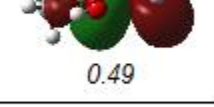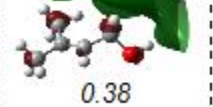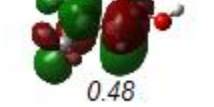
#	Alkene Name (ALK)	Abbreviation	Reference Probe	$k_{ALK+3BP*}$ (10^8 M^{-1} s^{-1})			
				Replicate 1	Replicate 2	Replicate 3	Average (SD)
1	5-Hexen-1-ol	5HxO	3MBO	3.1 (0.4)	1.9 (0.3)	2.2 (0.3)	2.4 (0.6)
2	Allyl alcohol	AlO	BDO	2.8 (0.3)	2.5 (0.2)	2.8 (0.3)	2.7 (0.2)
3	3-Hexene-1,6-diol	HDO	3MBO	2.5 (0.4)	3.7 (0.5)	3.2 (0.4)	3.1 (0.7)
4	2,3-Butadien-1-ol	BDO	3MBO	3.3 (0.5)	3.8 (0.5)	3.6 (0.5)	3.6 (0.3)
5	3-Buten-1-ol	3B1O	cHxO	4.2 (0.4)	3.2 (0.3)	3.6 (0.4)	3.7 (0.5)
6	1-Penten-3-ol	PE3O	3B2O	3.9 (1.1)	4.2 (1.2)	4.7 (1.3)	4.3 (0.4)
7	3-Buten-2-ol	3B2O	cHxO	5.7 (0.5)	5.6 (0.5)	3.3 (0.5)	4.9 (1.3)
8	2-Buten-1-ol	2B1O	4M3PO	5.6 (0.2)	4.1 (0.3)	5.9 (0.5)	5.2 (1.0)
9	5-Hexenyl acetate	5HxAc	3MBO	4.7 (0.7)	5.0 (0.7)	7.9 (1.1)	5.9 (1.8)
10	trans-3-hexen-1-ol	tHxO	3MBO	13 (2)	14 (2)	14 (2)	14 (1)
11	1-Chloro-3-methyl-2-butene	CMB	BDO [a]	17 (1)	-	-	17 (1)[b]
12	3-Methyl-2-buten-1-ol	3MBO	cHxO	21 (2)	20 (2)	16 (1)	19 (3)
13	2-Methyl-2-penten-1-ol	2M2PO	3MBO	29 (4)	28 (4)	28 (4)	28 (1)
14	4-Methyl-3-penten-1-ol	4M3PO	3MBO	42 (6)	39 (5)	40 (5)	40 (2)
15	cis-3-hexen-1-ol	cHxO	PhOH	62 (11)[c]	70 (13)	59 (11)	64 (6)
16	cis-3-hexenyl acetate	cHxAc	cHxO	66 (7)	71 (6)	59 (5)	65 (6)
17	Methyl jasmonate	MeJA	cHxO	80 (7)	69 (6)	75 (7)	75 (5)

[a] Measurement of the rate constant for CMB was done in a solution containing a minimal amount of acetonitrile to dissolve the compound.

[b] Error represents ± 1 SE, based on the SE of the relative rate slope and reference rate constant $k_{BDO+3BP*}$ given in the table.

[c] Phenol (PhOH) was used as the reference probe using the reference rate constant of 3.9 (± 0.7) × 10^9 M^{-1} s^{-1}, measured in this study, using 2,4,6,-trimethylphenol (TMP) as a reference compound ($k_{TMP+3BP*}$ = 5.1 (± 0.9) × 10^9 M^{-1} s^{-1}; Canonica et al. (2000)).

29   **Table S2.** Highest- and singly-occupied molecular orbitals (HOMOs, SOMOs) of representative alkenes
30   showing removing of an electron from the π system.[†]

ALK Abbreviation (#)	HOMO	SOMO	HOMO+1 (eV)	SOMO+1 (eV)
HDO (3)			0.39	0.45
BDO (4)			0.41	0.45
PE3O (6)			0.41	0.49
3B2O (7)			0.40	0.49
3MBO (12)			0.38	0.48
cHxO (15)			0.39	0.46

31
32 [†] HOMOs and SOMOs were computed from single point calculations at MP2/CBSB3 (Frisch et al.,
33 2016). HOMO+1 and SOMO+1values in eV are shown relative to HOMO and SOMO, respectively.

34 **Table S3.** HOMOs and SOMOs of alkenes showing removing of an electron from the oxygen.[†]

ALK Abbreviation (#)	HOMO	SOMO	HOMO+1 (eV)	SOMO+1 (eV)
3B1O (5)			*0.40*	*0.45*
HxAc (16)			*0.39*	*0.44*
MeJA (17)			*0.37*	*0.19*

[†]HOMOs and SOMOs were computed from single point calculations at MP2/CBSB3 (B3LYP/CBSB7 was used for ALKs 35 **16** and **17**). HOMO+1 and SOMO+1 values in eV are shown relative to HOMO and SOMO, respectively.

36 **Table S4.** Oxidation potentials (in units of V) of various isomers of isoprene- and limonene-derived
37 OVOCs, calculated using the CBS-QB3 compound method. The lowest energy isomer for each OVOC
38 is highlighted using a blue box. Compounds not shown here (18, 20 and 22) have no relevant isomers.

δ4 ISOPOOH (19)	δISONO2 (21)	LMNALD (23)	2,5OH-LMNALD (24)		4,7OH-LMNALD (25)
2.25	2.40	2.22	2.06	2.24	2.17
2.28	2.45	2.28	2.12	2.26	2.17
			2.23	2.39	2.21
			2.24	2.39	2.41
					2.48

39

5

40 **Table S5.** Measured or estimated rate constants for reactions of OVOCs with oxidants, photolysis, and hydrolysis.

OVOC		Gas-phase rate constants (cm^3 mlc^{-1} s^{-1})					
#	Name	$k_{OVOC+OH}$	Reference	$k_{OVOC+O3}$	Reference	$j_{Photolysis}$ (s^{-1})	Reference
18	β4-ISOPOOH	1.2E-10	St. Clair et al. (2015)	1.3E-17	Khamaganov and Hites (2001)		
19	δ4-ISOPOOH	1.2E-10	St. Clair et al. (2015)	1.3E-17	Khamaganov and Hites (2001)		
20	β-ISONO2	5.4E-11	Lee et al. (2014)	5.0E-19	Lee et al. (2014)		
21	δ-ISONO2	1.1E-10	Lee et al. (2014)	2.8E-17	Lee et al. (2014)		
22	HPALD2	5.1E-11	Wolfe et al. (2012)	1.2E-18	Wolfe et al. (2012)	6.3E-05	Wolfe et al. (2012)
23	LMNALD	1.6E-10	Gill and Hites (2002)	2.1E-16	Khamaganov and Hites (2001)		
24	2,5OH-LMNALD	1.6E-10	Gill and Hites (2002)	2.1E-16	Khamaganov and Hites (2001)		
25	4,7OH-LMNALD	1.6E-10	Gill and Hites (2002)	2.1E-16	Khamaganov and Hites (2001)		
26	HPALD1	5.1E-11	Wolfe et al. (2012)	1.2E-18	Wolfe et al. (2012)	6.3E-05	Wolfe et al. (2012)
OVOC		Aqueous-phase rate constants (L mol^{-1} s^{-1})					
#	Name	$k_{OVOC+OH}$	Reference	$k_{OVOC+O3}$	Reference	$k'_{Hydrolysis}$ (s^{-1})	Reference
18	β4-ISOPOOH	2.5E+09	Rivera-Rios et al. (2018)	4.7E+04	Schöne and Herrmann (2014) [a]		
19	δ4-ISOPOOH	2.5E+09	Rivera-Rios et al. (2018)	4.7E+04	Schöne and Herrmann (2014) [a]		
20	β-ISONO2	5.0E+09	Herrmann et al. (2015) [b]	4.7E+04	Schöne and Herrmann (2014) [a]	1.6E-05	Jacobs et al. (2014)
21	δ-ISONO2	5.0E+09	Herrmann et al. (2015) [b]	4.7E+04	Schöne and Herrmann (2014) [a]	6.8E-03	Jacobs et al. (2014)
22	HPALD2	9.0E+09	Schöne et al. (2014) [c]	2.3E+04	Schöne and Herrmann (2014) [c]		
23	LMNALD	1.0E+10	Witkowski et al. (2018) [d]	4.0E+04	Witkowski et al. (2018) [d]		
24	2,5OH-LMNALD	1.0E+10	Witkowski et al. (2018)	4.0E+04	Witkowski et al. (2018) [d]		
25	4,7OH-LMNALD	1.0E+10	Witkowski et al. (2018) [d]	4.0E+04	Witkowski et al. (2018) [d]		
26	HPALD1	9.0E+09	Schöne et al. (2014) [c]	2.3E+04	Schöne and Herrmann (2014) [c]		

41 [a] Average of rate constants for methacrolein and methyl vinyl ketone used as a proxy.

42 [b] Estimate based on the rate constants for similar unsaturated compounds with •OH in the indicated reference.

43 [c] Rate constant for methacrolein used as a proxy.

44 [d] Rate constants for neutral dicarbonyl derivatives of limonic and limononic acids, used a proxies.

Table S6. Loss rate constants for OVOCs due to different pathways.

#	OVOC Name	K_H[a] (M atm^{-1})	χ_{aq}[b]	$k'_{OH,g}$[c]	$k'_{O3,g}$[d]	j_{hv}[e]	$k'_{OH,aq}$[f]	$k'_{O3,aq}$[g]	$k'_{3BP*,aq}$[h] (High Triplet Reactivity)	$k'_{3C*,aq}$[i] (Typical Triplet Reactivity)	k'_{Hyd}[j]
				Pseudo-first-order rate constant for loss due to oxidants in the gas-phase (s^{-1})			Pseudo-first-order rate constant for loss due to oxidants in the aqueous-phase (s^{-1})				
18	β4-ISOPOOH	1.5E+06	0.97	1.2E-04	9.6E-06		5.0E-06	1.6E-05	4.0E-06	1.4E-07	
19	δ4-ISOPOOH	1.2E+06	0.97	1.2E-04	9.6E-06		5.0E-06	1.6E-05	6.8E-05	2.4E-06	
20	β-ISONO2	5.1E+04	0.55	5.4E-05	3.7E-07		1.0E-05	1.6E-05	2.1E-05	7.3E-07	1.6E-05
21	δ-ISONO2	4.3E+04	0.51	1.1E-04	2.1E-05		1.0E-05	1.6E-05	4.6E-05	1.6E-06	6.8E-03
22	HPALD2	1.2E+05	0.75	5.1E-05	8.9E-07	6.3E-05	1.8E-05	7.6E-06	2.0E-05	7.0E-07	
23	LMNALD	4.5E+03	0.10	1.6E-04	1.6E-04		2.0E-05	1.3E-05	8.3E-05	2.9E-06	
24	2,5OH-LMNALD	8.0E+05	0.95	1.6E-04	1.6E-04		2.0E-05	1.3E-05	7.3E-05	2.6E-06	
25	4,7OH-LMNALD	8.0E+05	0.95	1.6E-04	1.6E-04		2.0E-05	1.3E-05	4.4E-05	1.6E-06	
26	HPALD1	1.2E+05	0.75	5.1E-05	8.9E-07	6.3E-05	1.8E-05	7.6E-06	-[k]	-[k]	

[a] Henry's law constants calculated using EPISuite version 4.1 (US EPA. Estimation Programs Interface Suite™ for Microsoft® Windows v 4.1, 2016).

[b] Fraction of OVOC in the aqueous phase, calculated as $\chi_{aq} = 1/(1+1/(K_H \times L \times R \times T))$, where K_H is the Henry's law constant of the OVOC, L is the assumed liquid water content (1×10^{-6} L-aq/L-g), R is the universal gas constant (0.082 L atm K^{-1} mol^{-1}), and $T = 298$ K.

[c,d,f,g,h,i] Pseudo-first-order rate constant for loss of OVOC due to oxidation by the given oxidant in the gas or aqueous phase, calculated by multiplying the bimolecular reaction rate constant (Table S6) with the corresponding steady-state concentration of the oxidant: [•OH(g)] = 1×10^6 molecules cm^{-3}, [O_3(g)] = 30 ppbv = 7.4×10^{11} molecules cm^{-3}, [•OH(aq)] = 2×10^{-15} M (estimate in typical fog drops, includes gas-to-aqueous partitioning, Kaur and Anastasio (2017)). [O_3(aq)] = 3.3×10^{-10} M (based on 30 ppbv O_3(g) and $K_H = 1.1 \times 10^{-2}$ M atm^{-1}; Seinfeld and Pandis (2012), and [^{3}C*(aq)] = 5×10^{-14} M (average concentration measured in Davis fog, Kaur and Anastasio (2017)).

[h] Pseudo-first-order rate constant for loss of OVOC due to oxidation by highly reactive triplets such as ^{3}BP*. This was calculated using the predicted second-order rate constants $k_{OVOC+3BP*}$ (Table 1, main text) and [^{3}C*(aq)] given in the footnote above.

[i] Pseudo-first-order rate constant for loss of OVOC due to oxidation by triplets of typical reactivity as measured in fog and particles in Davis, CA (Kaur and Anastasio, 2017; Kaur and Anastasio, 2018). To estimate these rate constants we multiplied the predicted second-order rate constants with ^{3}BP* ($k_{OVOC+3BP*}$) by a factor of 0.04, which is the ratio of the average of the rate constants of reaction of MeJA with ^{3}3MAP* and ^{3}DMB* (2.7×10^8 M^{-1} s^{-1}, Table S8) divided by the rate constant for MeJA with ^{3}BP* (7.5×10^9 M^{-1} s^{-1}, Tables S1 and S8).

[e,j] First-order rate constants for gas-phase photolysis and aqueous hydrolysis of the OVOC, respectively (also given in Table S5).

[k] The value of $k_{ALK+3BP*}$ for HPALD1 could not be determined due to challenges with calculating its oxidation potential. Because the CB3-QB3 method scales at N^7 (where N is the number of atoms), the larger compound required more computational power than available.

7

Table S7. OVOC lifetimes and fractions lost due to various pathways.

High Triplet Reactivity Scenario		Total		Fraction of OVOC lost due to each pathway [c]						
#	OVOC Name	k'_{OVOC} [a] (s^{-1})	τ [b] (h)	$^{\bullet}OH(g)$	$O_3(g)$	$h\nu(g)$	$^{\bullet}OH(aq)$	$O_3(aq)$	$^3BP^*(aq)$	Hyd(aq)
18	β4-ISOPOOH	2.7E-05	10	13%	1.0%	0%	18%	54%	14%	0%
19	δ4-ISOPOOH	9.0E-05	3.1	3.9%	0.32%	0%	5.4%	17%	74%	0%
20	β-ISONO2	5.9E-05	4.7	41%	0.28%	0%	9.4%	15%	19%	15%
21	δ-ISONO2	3.6E-03	0.078	1.5%	0.29%	0%	0.14%	0.22%	0.66%	97%
22	HPALD2	6.3E-05	4.4	20%	0.35%	25%	21%	9.1%	24%	0%
23	LMNALD	3.0E-04	0.93	49%	47%	0%	0.67%	0.44%	2.8%	0%
24	2,5OH-LMNALD	1.2E-04	2.4	6.9%	6.7%	0%	16%	11%	59%	0%
25	4,7OH-LMNALD	8.9E-05	3.1	9.0%	8.8%	0%	21%	14%	47%	0%
26	HPALD1	4.8E-05	5.8	27%	0.46%	33%	28%	12%	- [d]	0%
Typical Triplet Reactivity Scenario		Total		Fraction of OVOC lost due to each pathway [c]						
#	OVOC Name	k'_{OVOC} (s^{-1})	τ (h)	$^{\bullet}OH(g)$	$O_3(g)$	$h\nu(g)$	$^{\bullet}OH(aq)$	$O_3(aq)$	$^3C^*(aq)$	Hyd(aq)
18	β4-ISOPOOH	2.4E-05	12	15%	1.2%	0%	20%	63%	0.58%	0%
19	δ4-ISOPOOH	2.6E-05	11	14%	1.1%	0%	19%	58%	9.0%	0%
20	β-ISONO2	4.8E-05	5.8	51%	0.43%	0%	12%	18%	0.84%	18%
21	δ-ISONO2	3.5E-03	0.079	1.5%	0.29%	0%	0.14%	0.22%	0.02%	98%
22	HPALD2	4.8E-05	5.7	26%	0.46%	33%	28%	12%	1.1%	0%
23	LMNALD	2.9E-04	1.0	50%	49%	0%	0.69%	0.45%	0.10%	0%
24	2,5OH-LMNALD	5.0E-05	5.6	16%	16%	0%	38%	25%	4.9%	0%
25	4,7OH-LMNALD	4.9E-05	5.7	16%	16%	0%	39%	26%	3.0%	0%
26	HPALD1	4.8E-05	5.8	27%	0.46%	33%	28%	12%	- [d]	0%

[a] Total pseudo-first order rate constant for loss of OVOC, calculated as $k'_{OVOC} = \Sigma(\chi_{aq} \times k'_{Ox,aq} + (1-\chi_{aq}) \times k'_{Ox,gas})$. All pseudo-first-order rate constants ($k'_{Ox,aq}$, $k'_{Ox,gas}$, $j_{h\nu}$, k'_{Hyd}) are given in Table S6.

[b] Total lifetime of OVOC, calculated as $1/k'_{OVOC}$.

[c] Fraction of OVOC lost due to each pathway, calculated as $(\chi_{aq} \times k'_{Ox,aq})/k'_{OVOC}$ for aqueous pathways and $((1-\chi_{aq}) \times k'_{Ox,gas})/k'_{OVOC}$ for gas-phase processes.

[d] We were unable to compute the oxidation potential for HAPLD1 (see footnote k in Table S6), and thus could not estimate its rate constant with triplets.

73   **Table S8.** Second-order rate constants for reaction of some alkenes with model triplet excited states.

ALK	$k_{ALK+3C*}$ $10^8\ M^{-1}\ s^{-1}$			Average $(k_{MeJA+33MAP*},\ k_{MeJA+3DMB*})\ /\ k_{MeJA+3BP*}$ [c]
	[3]3MAP*	[3]DMB*	[3]BP*	
cHxO (**15**)	1.1 (± 0.2) [a]	0.24 (± 0.10) [a]	64 (± 6) [b]	0.010
cHxAc (**16**)	7.9 (± 2.0) [a]	15 (± 4) [a]	65 (± 6) [b]	0.18
MeJA (**17**)	1.2 (± 0.3) [a]	4.1 (± 1.6) [a]	75 (± 5) [b]	0.035 [d]

74   [a] Rate constants from Richards-Henderson et al. (2014). Listed uncertainties are ± 1 standard errors.
75   [b] Rate constants measured in this work (also shown in Table S1). Listed uncertainties here are ± 1 standard
76   deviation, n = 3.
77   [c] The ratio of the average bimolecular rate constants for reaction of MeJA with model triplets [3]3MAP* and
78   [3]DMB* to the rate constant for MeJA with [3]BP*.
79   [d] This is the rate constant ratio for MeJA as well as the median value of the rate constant ratio (see footnote *a*)
80   for the three alkenes.
81

82

83
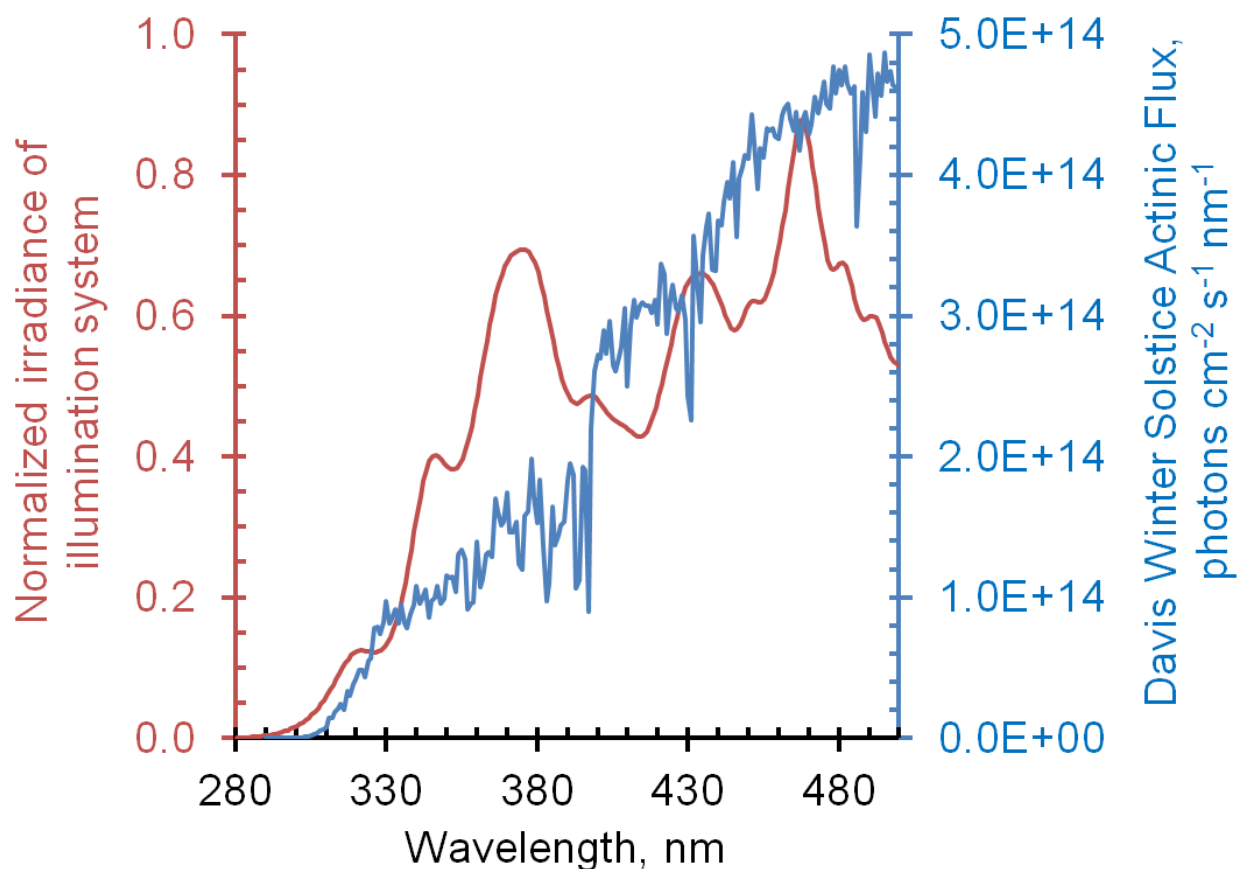
Figure S1. Comparison of the normalized irradiance from our illumination system (red line) and Davis, midday, winter solstice sunlight from the TUV model (blue line; Madronich et al. (2002)). Our illumination system irradiance was measured using a TIDAS spectrophotometer (counts cm^{-2} nm^{-1} s^{-1}) and normalized so that the area under its curve is equal to the area under the TUV actinic flux curve. Input parameters for the TUV model were: solar zenith angle: 62°, measurement altitude: 0 km, surface albedo: 0.1, aerosol optical depth: 0.235, cloud optical depth: 0.00.

91
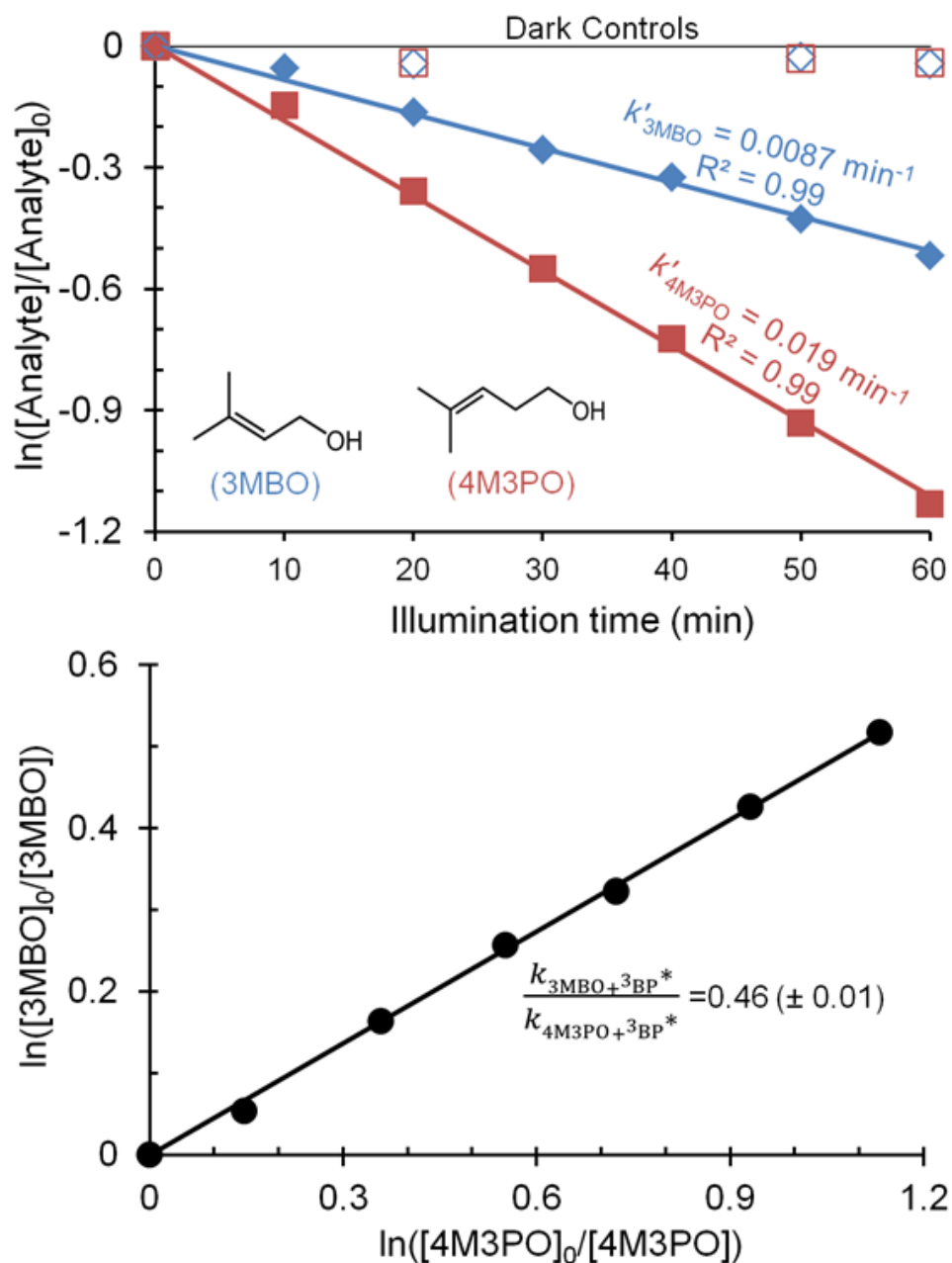
Figure S2. Illustration of the relative rate technique used for measuring rate constants (Finlayson-Pitts and Pitts Jr, 1999; Richards-Henderson et al., 2014). Top panel: Aqueous loss of the alkene (4M3PO) and reference compound (3MBO) in the presence of the BP triplet under solar simulated light (298 K, pH 5.5 (± 0.2)). Bottom panel: Plot of change in concentration of reference compound against alkene. The slope represents the ratio (± 1 SE) of the bimolecular rate constants with the BP triplet.

100

101
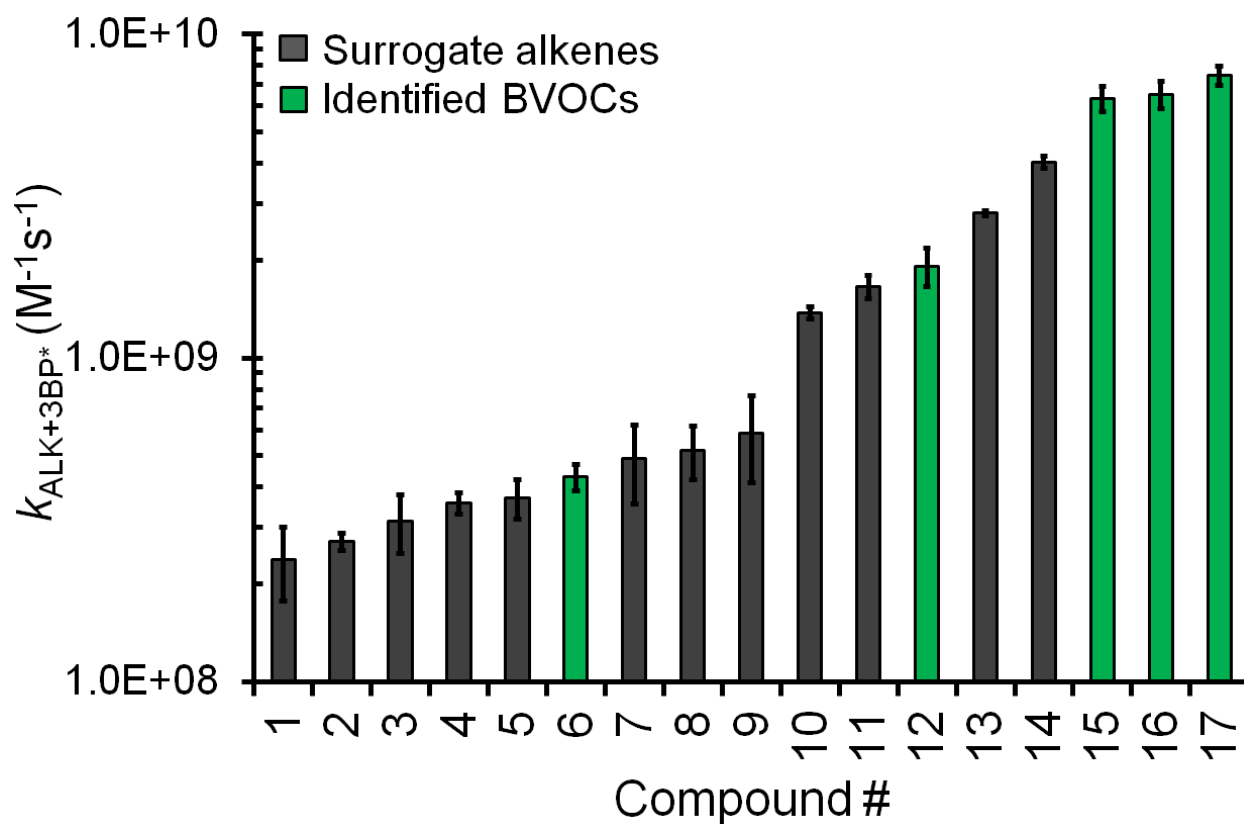
Figure S3. Measured bimolecular rate constants of 17 alkenes with triplet benzophenone. Green bars represent biogenic volatile organic compounds known to be emitted from plants; grey bars represent other C_3–C_6 alkenes. Error bars represent ±1 standard deviation (n = 3) except for compound 11, where n = 1 and the error is ± 1 SE (see Table S1 for details). Experimental conditions: 298 K, pH 5.5 ± 0.2, 1.0 mM phosphate buffer).
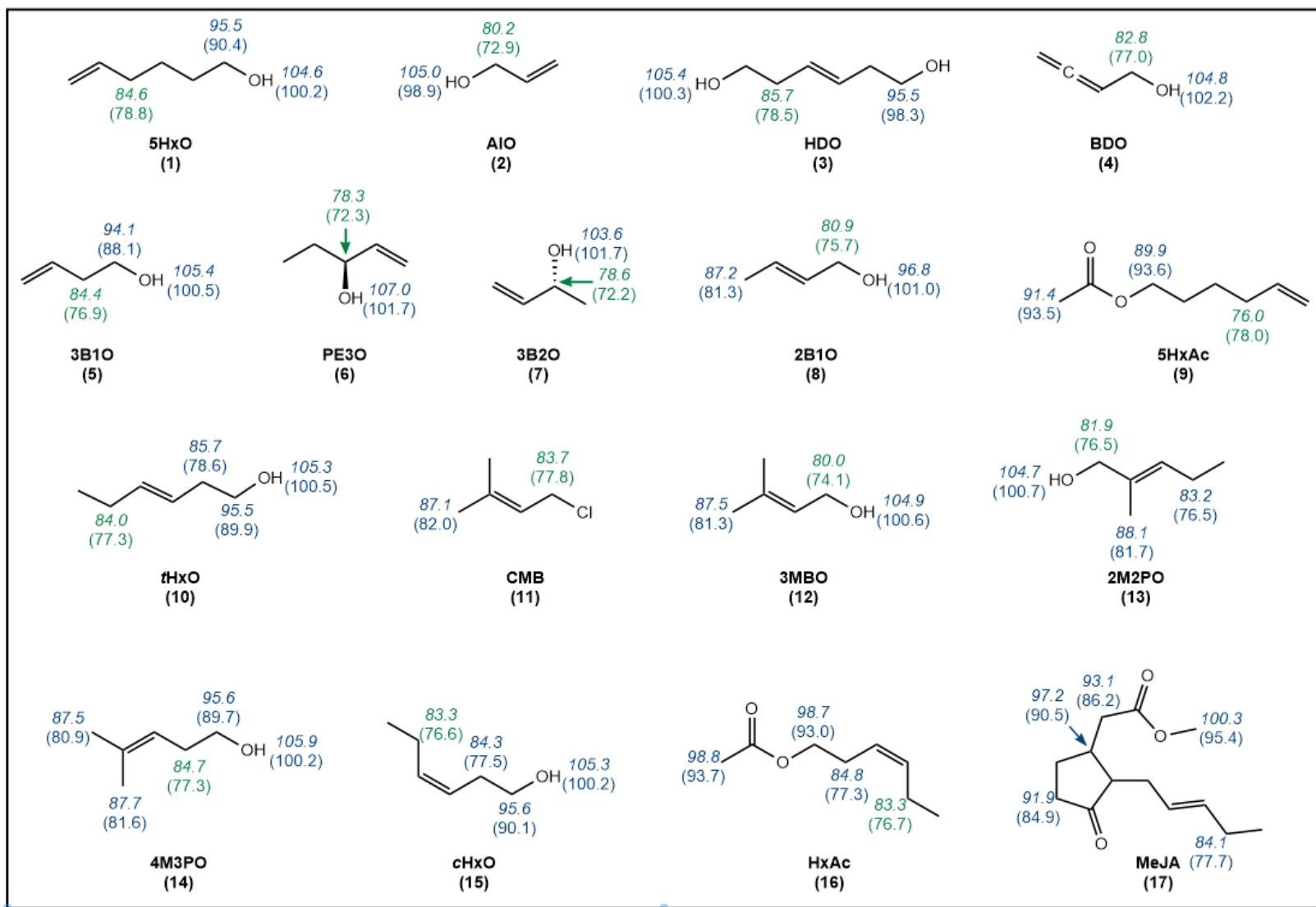
Figure S4. Bond dissociation enthalpies (in italics) and bond dissociation free energies (in parentheses) in kcal mol^{-1} for various hydrogens in each alkene. For each compound the hydrogen most likely to be abstracted, i.e., with the lowest bond dissociation energy, is shown in green.
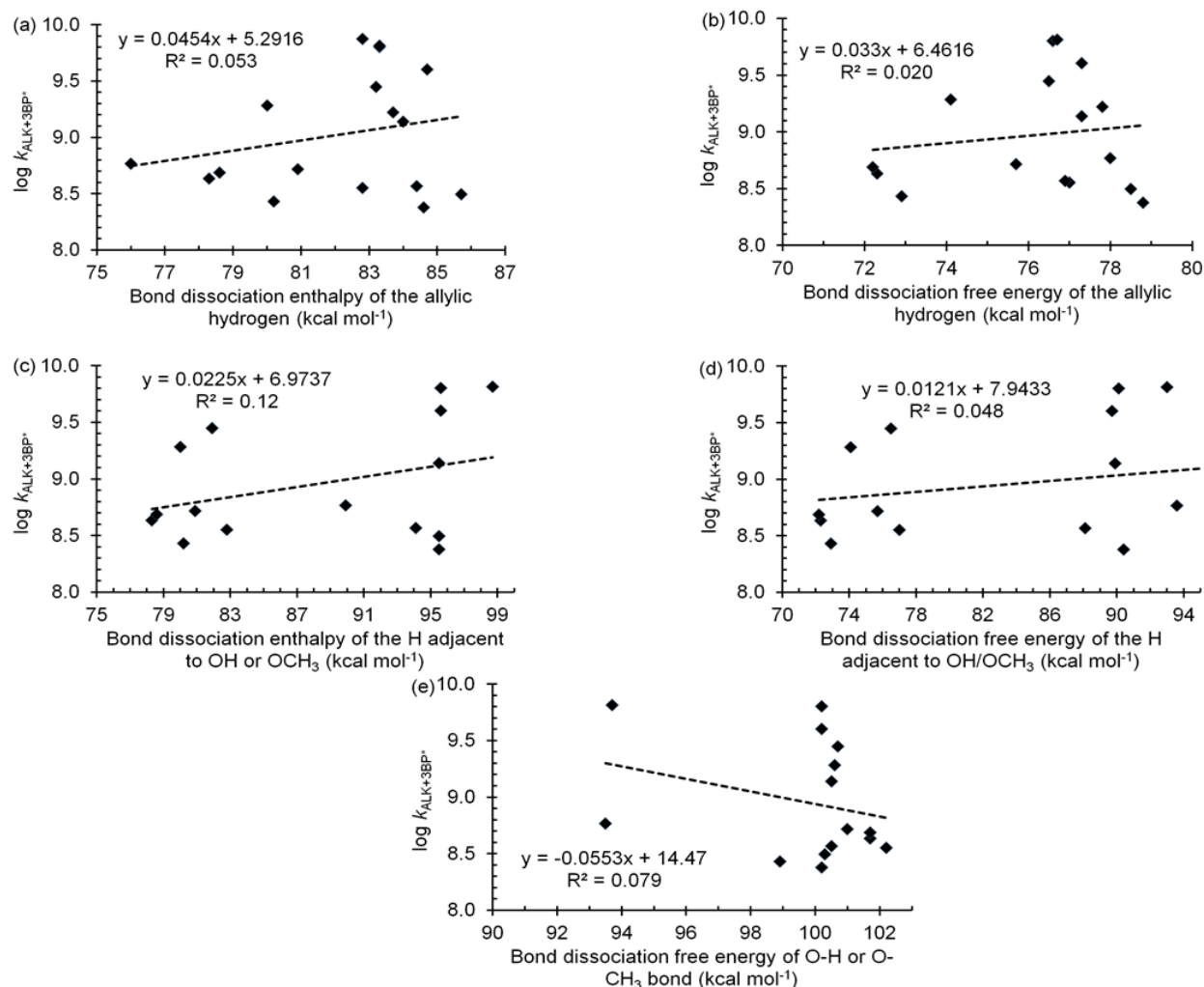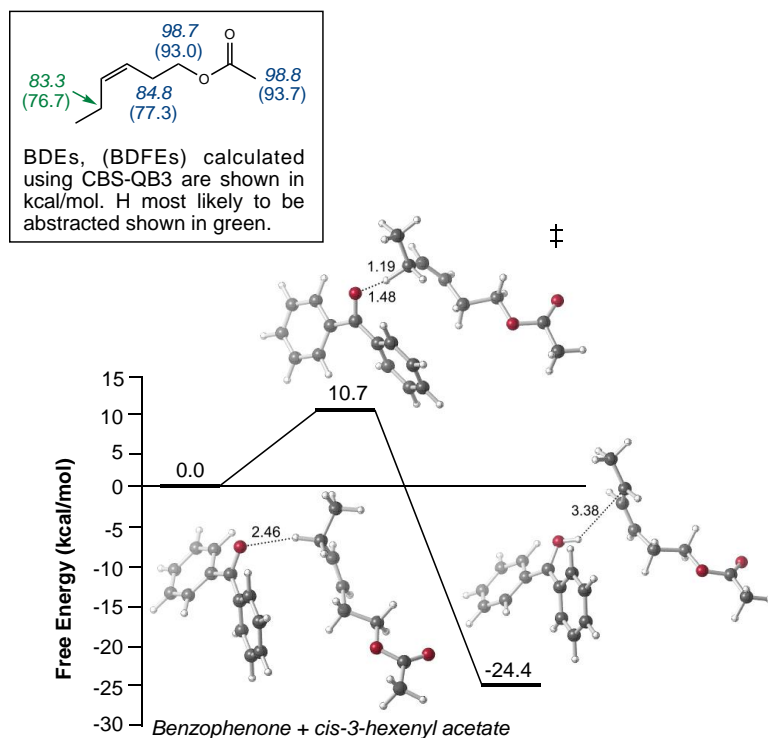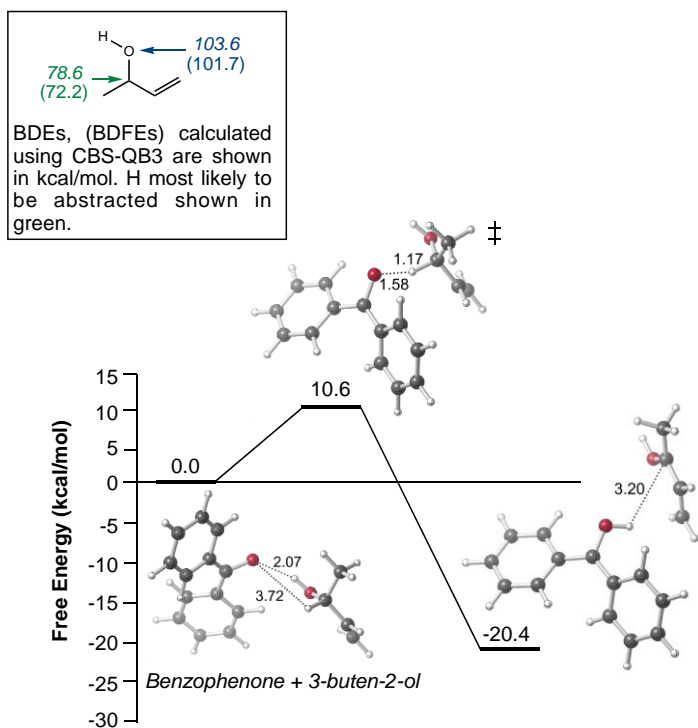
Figure S5. Correlation plots for measured rate constants and various computed bond dissociation energies. (a) Log $k_{ALK+3BP*}$ versus the lowest bond dissociation enthalpy of the allylic hydrogen in each alkene (i.e., the green values in Fig. S4). (b) Log $k_{ALK+3BP*}$ versus the lowest bond dissociation free energy of the allylic hydrogen. (c) Log $k_{ALK+3BP*}$ versus the bond dissociation enthalpy of the hydrogen attached to the carbon adjacent to the –OH or –OCH$_3$ group. (d) Log $k_{ALK+3BP*}$ versus the bond dissociation free energy of the hydrogen attached to the carbon adjacent to the –OH or –OCH$_3$ group. (e): log $k_{ALK+3BP*}$ versus bond dissociation free energy of the O-H or OH$_2$C-H bond. Bond dissociation energies are shown in Fig. S4.

14
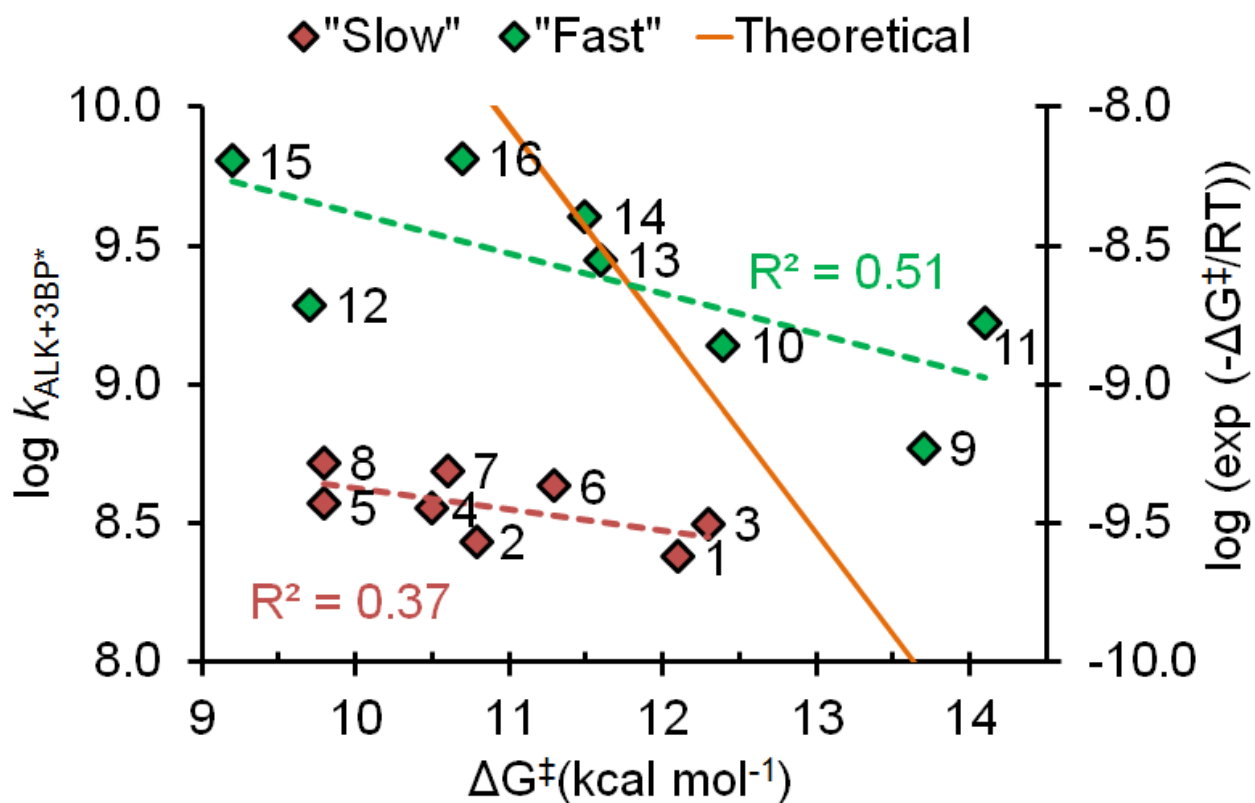
Figure S6. Log $k_{ALK+3BP*}$ versus lowest transition state free energy barrier. The alkenes are broken down into two groups: $k_{ALK+3BP*} < 5 \times 10^8$ M^{-1} s^{-1} (slow, red) and $k_{ALK+3BP*} \geq 5 \times 10^8$ M^{-1} s^{-1} (fast, green). The slopes ($\pm$ 1 SE) of these lines are $- 0.077$ ($\pm$ 0.041) and $- 0.15$ ($\pm$ 0.06) mol kcal^{-1}, respectively. Transition state energy barrier values are given in Table 1 of the main text. The orange line (plotted on the secondary y-axis) shows the trend in k values expected from transition state theory ($k_{ALK+3BP*} = A \times \exp (-\Delta G^{\ddagger}/RT)$).

BDEs, (BDFEs) calculated using CBS-QB3 are shown in kcal/mol. H most likely to be abstracted shown in green.

Benzophenone + 3-buten-2-ol

BDEs, (BDFEs) calculated using CBS-QB3 are shown in kcal/mol. H most likely to be abstracted shown in green.
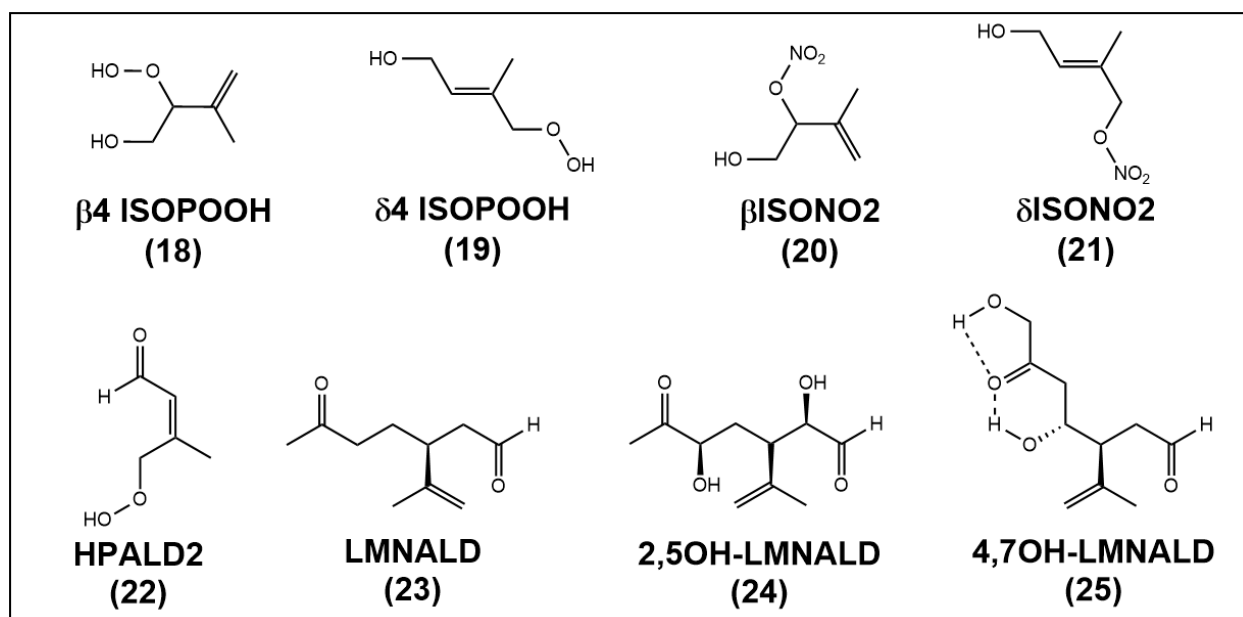
Benzophenone + cis-3-hexenyl acetate

128

129 **Figure S7.** Lowest transition state energy barriers for two alkenes: **7**, 3B2O, in the top panel and
130 **16**, cHxAc, in the bottom panel. Both show the hydrogen most likely to be abstracted during
131 oxidation; in both cases this is an allylic H.

132

133
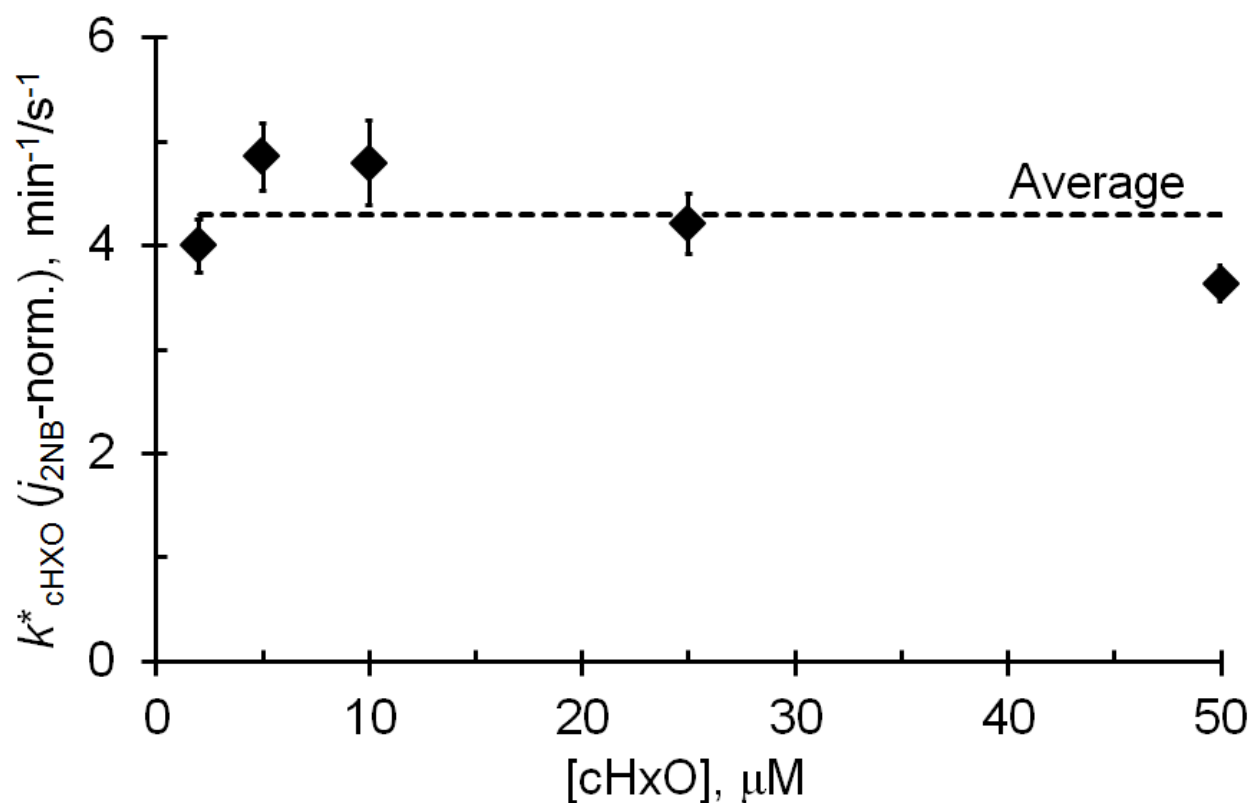
Figure S8. Pseudo-first-order loss rate constant of cHxO (k^*_{cHxO}) as a function of the concentration of cHxO. Since these experiments were performed on different days, the values are normalized to the photon flux of the illumination system on the day of the experiment by dividing by j_{2NB} (details in Kaur and Anastasio (2017)). The average (± 1 σ) value is 4.3 ± 0.5 min^{-1}/s^{-1}, giving a relative standard deviation of 12 %.

17

β4 ISOPOOH (18)   **δ4 ISOPOOH (19)**   **βISONO2 (20)**   **δISONO2 (21)**

HPALD2 (22)   **LMNALD (23)**   **2,5OH-LMNALD (24)**   **4,7OH-LMNALD (25)**

Figure S9. Lowest energy isomers of isoprene- and limonene-derived OVOCs, determined with gas-phase calculations using the CBS-QB3 compound method.

References

Canonica, S., Hellrung, B., and Wirz, J.: Oxidation of phenols by triplet aromatic ketones in aqueous solution, J. Phys. Chem. A, 104, 1226-1232, 2000.

Finlayson-Pitts, B. J., and Pitts Jr, J. N.: Chemistry of the Upper and Lower Atmosphere: Theory, Experiments, and Applications, Academic press, 1999.

Frisch, M., Trucks, G., Schlegel, H., Scuseria, G., Robb, M., Cheeseman, J., Scalmani, G., Barone, V., Petersson, G., Nakatsuji, H., Li, X., Caricato, M., Marenich, A., Bloino, J., Janesko, B., Gomperts, R., Mennucci, B., Hratchian, H., Ortiz, J., Izmaylov, A., Sonnenberg, J., Williams-Young, D., Ding, F., Lipparini, F., Egidi, F., Goings, J., Peng, B., Petrone, A., Henderson, T., Ranasinghe, D., Zakrzewski, V. G., Gao, J., Rega, N., Zheng, G., Liang, W., Hada, M., Ehara, M., Toyota, K., Fukuda, R., Hasegawa, J., Ishida, M., Nakajima, T., Honda, Y., Kitao, O., Nakai, H., Vreven, T., Throssell, K., J. A. Montgomery, J., Peralta, J. E., Ogliaro, F., Bearpark, M., Heyd, J. J., Brothers, E., Kudin, K. N., Staroverov, V. N., Keith, T., Kobayashi, R., Normand, J., Raghavachari, K., Rendell, A., Burant, J. C., Iyengar, S. S., Tomasi, J., Cossi, M., Millam, J. M., Klene, M., Adamo, C., Camml, R., Ochterski, J. W., Martin, R. L., Morokuma, K., Farkas, O., JB, F., and DJ, F.: Gaussian 09, Revision D.01; Gaussian: Wallingford, CT, USA, 2016,

Gill, K. J., and Hites, R. A.: Rate constants for the gas-phase reactions of the hydroxyl radical with isoprene, α-and β-pinene, and limonene as a function of temperature, The Journal of Physical Chemistry A, 106, 2538-2544, 2002.

Herrmann, H., Schaefer, T., Tilgner, A., Styler, S. A., Weller, C., Teich, M., and Otto, T.: Tropospheric aqueous-phase chemistry: Kinetics, mechanisms, and its coupling to a changing gas phase, Chem. Rev., 115, 4259-4334, 2015.

Jacobs, M. I., Burke, W., and Elrod, M. J.: Kinetics of the reactions of isoprene-derived hydroxynitrates: gas phase epoxide formation and solution phase hydrolysis, Atmos. Chem. Phys., 14, 8933-8946, 2014.

Kaur, R., and Anastasio, C.: Light absorption and the photoformation of hydroxyl radical and singlet oxygen in fog waters, Atmos. Environ., 164, 387-397, 2017.

Kaur, R., and Anastasio, C.: First Measurements of Organic Triplet Excited States in Atmospheric Waters, Environ. Sci. Technol., 52, 5218-5226, 2018.

Khamaganov, V. G., and Hites, R. A.: Rate Constants for the Gas-Phase Reactions of Ozone with Isoprene, α-and β-Pinene, and Limonene as a Function of Temperature, The Journal of Physical Chemistry A, 105, 815-822, 2001.

Lee, L., Teng, A. P., Wennberg, P. O., Crounse, J. D., and Cohen, R. C.: On Rates and Mechanisms of OH and O_3 Reactions with Isoprene-Derived Hydroxy Nitrates, The Journal of Physical Chemistry A, 118, 1622-1637, 2014.

Madronich, S., Flocke, S., Zeng, J., Petropavlovskikh, I., and Lee-Taylor, J.: Tropospheric Ultraviolet-Visible Model (TUV) version 4.1, National Center for Atmospheric Research, PO Box, 3000, 2002.

Richards-Henderson, N. K., Pham, A. T., Kirk, B. B., and Anastasio, C.: Secondary organic aerosol from aqueous reactions of green leaf volatiles with organic triplet excited states and singlet molecular oxygen, Environ. Sci. Technol., 49, 268-276, 2014.

Rivera-Rios, J. C., Zhao, R., Lee, A. K. Y., Abbatt, J. P. D., Crounse, J. D., Compernolle, S., Wennberg, P. O., and Keutsch, F. N.: In Preparation, 2018.

Schöne, L., and Herrmann, H.: Kinetic measurements of the reactivity of hydrogen peroxide and ozone towards small atmospherically relevant aldehydes, ketones and organic acids in aqueous solutions, Atmos. Chem. Phys., 14, 4503, 2014.

Schöne, L., Schindelka, J., Szeremeta, E., Schaefer, T., Hoffmann, D., Rudzinski, K. J., Szmigielski, R., and Herrmann, H.: Atmospheric aqueous phase radical chemistry of the isoprene oxidation products

189   methacrolein, methyl vinyl ketone, methacrylic acid and acrylic acid–kinetics and product
190   studies, Phys. Chem. Chem. Phys., 16, 6257-6272, 2014.
191 Seinfeld, J. H., and Pandis, S. N.: Atmospheric chemistry and physics: From air pollution to climate
192   change, John Wiley & Sons, 2012.
193 St. Clair, J. M., Rivera-Rios, J. C., Crounse, J. D., Knap, H. C., Bates, K. H., Teng, A. P., Jørgensen, S.,
194   Kjaergaard, H. G., Keutsch, F. N., and Wennberg, P. O.: Kinetics and Products of the Reaction of
195   the First-Generation Isoprene Hydroxy Hydroperoxide (ISOPOOH) with OH, The Journal of
196   Physical Chemistry A, 120, 1441-1451, 2015.
197 US EPA. Estimation Programs Interface Suite™ for Microsoft® Windows v 4.1: Estimation Programs
198   Interface Suite™ for Microsoft® Windows, v 4.1. United States Environmental Protection Agency,
199   Washington, DC, USA., 2016.
200 Witkowski, B., Al-sharafi, M., and Gierczak, T.: Kinetics of Limonene Secondary Organic Aerosol
201   Oxidation in the Aqueous Phase, Environmental science & technology, 52, 11583-11590, 2018.
202 Wolfe, G. M., Crounse, J. D., Parrish, J. D., Clair, J. M. S., Beaver, M. R., Paulot, F., Yoon, T. P., Wennberg,
203   P. O., and Keutsch, F. N.: Photolysis, OH Reactivity and Ozone Reactivity of a Proxy for Isoprene-
204   Derived Hydroperoxyenals (HPALDs), Phys. Chem. Chem. Phys., 14, 7276-7286, 2012.

205